

The retinoid X receptor: a nuclear receptor that modulates the sleep-wake cycle in rats

Eric Murillo-Rodríguez^{1,2} · Diana Millán-Aldaco³ · Gloria Arankowsky-Sandoval⁴ · Tetsuya Yamamoto^{2,5} · Luis Cid^{2,6} · Diogo Monteiro^{2,6} · Nuno Barbosa Rocha^{2,7} · Diogo Telles-Correia^{2,8} · Diogo S. Teixeira^{2,9} · André Barciela Veras^{2,10} · Henning Budde^{2,11} · Sérgio Machado^{2,12} · Claudio Imperatori^{2,13} · Pablo Torterolo^{2,14}

Received: 28 November 2019 / Accepted: 1 April 2020
© Springer-Verlag GmbH Germany, part of Springer Nature 2020

Abstract

Rationale The nuclear receptor retinoid X receptor (RXR) belongs to a nuclear receptor superfamily that modulates diverse functions via homodimerization with itself or several other nuclear receptors, including PPAR α . While the activation of PPAR α by natural or synthetic agonists regulates the sleep-wake cycle, the role of RXR in the sleep modulation is unknown.

Objectives We investigated the effects of bexarotene (Bexa, a RXR agonist) or *UVI 3003* (UVI, a RXR antagonist) on sleep, sleep homeostasis, levels of neurochemical related to sleep modulation, and *c-Fos* and NeuN expression.

Methods The sleep-wake cycle and sleep homeostasis were analyzed after application of Bexa or UVI. Moreover, we also evaluated whether Bexa or UVI could induce effects on dopamine, serotonin, norepinephrine epinephrine, adenosine, and acetylcholine contents, collected from either the nucleus accumbens or basal forebrain. In addition, *c-Fos* and NeuN expression in the hypothalamus was determined after Bexa or UVI treatments.

Results Systemic application of Bexa (1 mM, i.p.) attenuated slow-wave sleep and rapid eye movement sleep. In addition, Bexa increased the levels of dopamine, serotonin, norepinephrine epinephrine, adenosine, and acetylcholine sampled from either the nucleus accumbens or basal forebrain. Moreover, Bexa blocked the sleep rebound period after total sleep deprivation, increased in the hypothalamus the expression of *c-Fos*, and decreased NeuN activity. Remarkably, *UVI 3003* (1 mM, i.p.) induced opposite effects in sleep, sleep homeostasis, neurochemicals levels, and *c-Fos* and NeuN activity.

Conclusions The administration of RXR agonist or antagonist significantly impaired the sleep-wake cycle and exerted effects on the levels of neurochemicals related to sleep modulation. Moreover, Bexa or UVI administration significantly affected *c-Fos* and NeuN expression in the hypothalamus. Our findings highlight the neurobiological role of RXR on sleep modulation.

Keywords Adenosine · Dopamine · Retinoid X receptor · Serotonin · Sleep

✉ Eric Murillo-Rodríguez
eric.murillo@anahuac.mx

¹ Laboratorio de Neurociencias Moleculares e Integrativas, Escuela de Medicina, División Ciencias de la Salud, Universidad Anáhuac Mayab, Km. 15.5 Carretera Mérida-Progreso. Int. Km. 2 Carretera a Chablekal, C.P. 97308 Mérida, Yucatán, Mexico

² Intercontinental Neuroscience Research Group, Mérida, Mexico

³ Neurociencia Cognitiva, Instituto de Fisiología Celular, Universidad Nacional Autónoma de México, Mexico City, Mexico

⁴ Centro de Investigaciones Regionales “Dr. Hideyo Noguchi”, Universidad Autónoma de Yucatán, Mérida, Yucatán, Mexico

⁵ Graduate School of Technology, Industrial and Social Sciences, Tokushima University, Tokushima, Japan

⁶ Sport Science School of Rio Maior, Instituto Politécnico de Santarém, Santarém, Portugal

⁷ Health School, Polytechnic Institute of Porto, Porto, Portugal

⁸ Faculty of Medicine, University of Lisbon, Lisbon, Portugal

⁹ Faculdade de Educação Física e Desporto/Faculty of Physical Education and Sport, Universidade Lusófona de Humanidades e Tecnologias, Lisbon, Portugal

¹⁰ School of Medicine, State University of Mato Grosso do Sul, Campo Grande, Mato Grosso del Sur, Brazil

¹¹ Faculty of Human Sciences, Medical School Hamburg, Hamburg, Germany

¹² Salgado de Oliveira University, Niterói, Brazil

¹³ Department of Human Sciences, European University of Rome, Rome, Italy

¹⁴ Laboratorio de Neurobiología del Sueño, Departamento de Fisiología, Facultad de Medicina, Universidad de la República, Montevideo, Uruguay

Q4/Q3 33

Introduction

34 The nuclear receptor retinoid X receptor (RXR) belongs to a
 35 superfamily of nuclear receptors engaged in a wide variety of
 36 biological processes, including protective effects against neu-
 37 rodegenerative diseases (Casali et al., 2018; Loera-Valencia
 38 et al., 2019; Martin et al., 2019; Schierle and Merk, 2019;
 39 Simandi et al., 2018). The RXR can form both homodimer
 40 as well as heterodimer complexes with other nuclear recep-
 41 tors, such as the peroxisome proliferator-activated receptor
 42 alpha (PPAR α ; Kojetin et al., 2015; Lefebvre et al., 2010).
 43 The activation of PPAR α by natural or synthetic agonists en-
 44 gages gene expression and modulates diverse physiological
 45 and clinical conditions, such as cancer, cardiovascular disor-
 46 ders, autism, among others (Barone et al., 2019; Choi, 2019;
 47 Laleh et al., 2019; Mirza et al., 2019; Yamashita et al., 2019).
 48 Our group has demonstrated that modulation of PPAR α activ-
 49 ity by the synthetic agonist (Wy14643) or the antagonist (MK-
 50 886) exerts effects on the sleep-wake cycle and neurochemi-
 51 cals linked to sleep control (Mijangos-Moreno et al., 2016;
 52 Murillo-Rodríguez et al., 2016; Murillo-Rodríguez, 2017).

53 On the other hand, agonist or antagonists to RXR are used
 54 to explore the molecular mechanism of action in medical treat-
 55 ments (Martínez et al., 2019; Krężel et al., 2019; Schierle and
 56 Merk, 2019; Wnuk et al., 2018). In this regard, the RXR
 57 agonist bexarotene (Bexa) has been tested with positive results
 58 for the management of diabetes, cancer, and cardiovascular
 59 diseases (Geller et al., 2019; Guleria et al., 2013; Tu et al.,
 60 2018). Moreover, multiple pieces of evidence have demon-
 61 strated that Bexa shows neuroprotective properties against
 62 neurodegenerative diseases, including Alzheimer's disease,
 63 multiple sclerosis, and Parkinson's disease as well
 64 (Bartzokis, 2014; Fanaee-Danesh et al., 2019; McFarland
 65 et al., 2013). Whereas the molecular mechanism of action of
 66 Bexa remains to be described in detail, several docking exper-
 67 iments have shown that this drug activates various RXR re-
 68 ceptor isoforms (α , β , and γ) as a putative molecular pathway
 69 of activation (Nam et al., 2016; Dheer et al., 2018; Chitranshi
 70 et al., 2019).

71 Although limited, several antagonists to RXR have been
 72 recently studied, including *UVI 3003* (*UVI*; Clemens et al.,
 73 2018; Hebert et al., 2017; Mengeling et al., 2018; Watanabe
 74 and Kakuta, 2018) which, pharmacologically, behaves as a
 75 RXR pan antagonist acting on more than two isoforms (α
 76 and γ ; Watanabe and Kakuta, 2018; AlSudais et al., 2018).
 77 Despite that the role of PPAR α on sleep modulation has been
 78 explored, the role of RXR in sleep modulation is unknown.
 79 Furthermore, the effects of Bexa or UVI on sleep control have
 80 not been investigated. Thus, since Bexa activates PPAR α
 81 (Tuncan et al., 2018; Yu et al., 2015), then we have hypoth-
 82 esized that the sleep-wake cycle may be influenced by the
 83 RXR agonist. To achieve this aim, we investigated the in-
 84 volvement of Bexa or UVI in the control of the sleep-wake

cycle with focus on their role in sleep ad libitum and sleep 85
 homeostasis response. The effects of Bexa or UVI treatment 86
 on neurotransmitters, including dopamine, serotonin, norepi- 87
 nephrine epinephrine, adenosine, and acetylcholine, linked to 88
 sleep control were collected from either the nucleus accum- 89
 bens of the basal forebrain for further study. In addition, the 90
 activation of neurons has been associated with the activity of 91
 immediate expression genes, including *c-Fos* and NeuN (de- 92
 la-Cruz et al., 2018; Duan et al., 2016; Farivar et al., 2004; 93
 Gallo et al., 2018; Gusel'nikova and Korzhevskiy, 2015; 94
 Hight et al., 2010; Huang et al., 2019; Jaworski et al., 2018; 95
 Kovács, 2008). Thus, the present study also addressed the 96
 potentially effects of Bexa or UVI treatment in sleep-related 97
 brain area by addressing the *c-Fos* and NeuN expression in the 98
 hypothalamus. 99

Materials and methods 100

**Experiment 1: Bexarotene or UVI 3003 exert effects 101
 on sleep** 102

Ethics approval 103

104 The animal experimental procedures were performed in accor- 104
 dance with the domestic and international standards of Animal 105
 Welfare including the Mexican Standards Related to Use and 106
 Management of Laboratory Animals (DOF. NOM-062-Z00- 107
 1999), the National Institutes of Health (NIH Publication No. 108
 80-23, revised 1996), and the ARRIVE (Animal Research: 109
 Reporting of in vivo Experiments) guidelines, the commonly 110
 accepted "3Rs" Guidelines. Male Wistar rats from Animal 111
 Vivarium Center, Universidad Anáhuac Mayab, were used 112
 in this study. All the study was approved by the Research 113
 and Ethics Committee of Universidad Anáhuac Mayab 114
 (Mérida, Yucatán, México). For ethical reasons, the current 115
 report used a reduced number of animals. 116

Animals 117

118 Adult Male Wistar rats were used for the experiments ($N = 26$; 118
 250–280 g). Upon arrival to our laboratory, the animals were 119
 acclimatized to the experimental conditions and kept under a 120
 12-h light/dark cycle (lights on at 08:00 h; 200 lx), in a tem- 121
 perature (21 ± 1 °C), and humidity-controlled environment 122
 ($60 \pm 10\%$) with free access to food (Purina Rat Chow, 123
 Purina, México) as well as fresh tap water. 124

Chemicals and materials 125

126 Bexarotene (PubChem CID: 82146) and UVI 3003 126
 (PubChem CID: 44566108) were purchased from Sigma- 127
 Aldrich (St. Louis, MO, USA). Drug solutions were prepared 128

129 immediately before use in a vehicle (VEH) consisting of di-
 130 methyl sulfoxide (DMSO; PubChem CID: 679) followed by
 131 phosphate-buffered saline (10% DMSO final concentration;
 132 He et al., 2018; Dheer et al., 2019). All other chemicals and
 133 reagents were of analytical grade (Sigma-Aldrich, St. Louis,
 134 MO, USA). Sleep studies necessitated materials from Plastics
 135 One (Roanoke, VA, USA). Microdialysis experiments re-
 136 quired materials from Bioanalytical Systems (BAS, West
 137 Lafayette, IN, USA) whereas high-performance liquid chro-
 138 matography (HPLC) depended upon Shimadzu materials
 139 (Kyoto, Japan) and Merck Millipore (Darmstadt, Germany).
 140 The immunohistochemical analysis demanded reagents from
 141 Santa Cruz Biotechnology, Inc. (Dallas, TX, USA) and Vector
 142 Laboratories (Burlingame, CA, USA).

143 **Sleep-recording surgeries**

144 Rats ($n = 8$) were anesthetized (acepromazine [0.75 mg/kg],
 145 xylazine [2.5 mg/kg], and ketamine [22 mg/kg]; intraperito-
 146 neal [i.p.]) and placed in a stereotaxic frame (David Kopf
 147 Instruments, Tujunga, CA, USA) for implantation of epidural
 148 screw electrodes for recording of the electroencephalogram
 149 (EEG), and stainless-steel wires in the neck extensor muscles
 150 to record the electromyogram (EMG). The EEG/EMG elec-
 151 trode wires were inserted into a six-pin connector plastic plug
 152 (Plastics One, Roanoke, VA, USA) and attached onto the skull
 153 by using commercial dental cement. The connector was at-
 154 tached to a 50-cm recording cable (Plastics One, Roanoke,
 155 VA, USA) linked to a 6-channel slip-ring commutator
 156 (Plastics One, Roanoke, VA, USA) which allowed free mov-
 157 ing of animal around in the cage. Upon completion of the
 158 EEG/EMG surgeries, animals were placed into individual
 159 cages with free access to food and water (Murillo-Rodríguez
 160 et al., 2019).

161 **Habituation processes**

162 After EEG/EMG surgeries, animals were habituated to exper-
 163 imenters by daily 10 min of handling and removal from the
 164 sleep-recording system across 7 days. When signs of no stress
 165 (aggression, droppings, and/or urine) were observed when
 166 researcher handled the animals, the habituation period was
 167 considered complete.

168 **Drugs preparation and administrations**

169 Seven days after EEG/EMG surgeries (habituation/post-sur-
 170 gery recovery period), rats were randomly assigned to the
 171 following groups: control (vehicle [VEH]: DMSO and
 172 phosphate-buffered saline [10% DMSO final concentration]),
 173 bexarotene (Bexa), or UVI 3003 (UVI). The final concentra-
 174 tion of Bexa and UVI was the same (1 mM). The solutions of
 175 Bexa (5 mg/kg, i.p.) and UVI (3 mg/kg, i.p.) were injected as

reported by others (Dheer et al., 2019; He et al., 2018; Zhang 176
 et al., 2019). To avoid experimental biases, such as circadian 177
 influences in sleep results, the pharmacological challenges 178
 were given 1 h after the start of the beginning of either the 179
 lights-on or the lights-off period. In addition, one blind ob- 180
 server to the nature of treatments applied the administrations. 181
 Once experimental challenges were administered, rats were 182
 reattached to the sleep-recording system and sleep data were 183
 collected across the next 4 h. For ethical reasons, a reduced 184
 number of animals were used in the whole project. Thus, to 185
 achieve our experimental hypothesis, a Latin square crossover 186
 design was used then (Table 1). The Latin square is an experi- 187Q5
 mental design in which each treatment is assigned to a spe- 188
 cific period, with a defined number of interventions given to 189
 each subject. The carryover effects are controlled by using the 190
 Latin square experimental design that are “counterbalanced.” 191
 In addition, treatments were applied to rats with an interval 192
 between administrations of 48 h. 193

Analysis of sleep recordings 194

The EEG/EMG signals were scored in 12 s epochs and am- 195
 plified, filtered (70 Hz [low-pass filter] and 0.3 Hz [high-pass 196
 filter]; Model M15LT 15A54, Grass Instruments, Quincy, 197
 MA, USA), and digitized at a sampling rate of 128 Hz by 198
 using a 100-bit analog-to-digital converter board (NI PCI- 199
 6033E Multifunction I/O Board and NI-DAQ Software, 200
 SCB-100 Shielded Connector Block, National Instruments, 201
 Austin, TX, USA) recorded and visually scored with the 202
 ICELUS software. The EEG/EMG data were characterized 203Q6
 in wakefulness (W) when the presence of desynchronized 204
 EEG with high EMG activity was observed in sleep record- 205
 ings whereas the slow-wave sleep (SWS) defined as high- 206
 amplitude slow waves with a low EMG tone relative to W 207
 was found in the EEG/EMG charts. Lastly, rapid eye move- 208
 ment sleep (REMS) was identified by regular theta activity 209

Table 1 The Latin square design used in the current study. The Latin 1.1
 square design was a method used for placing treatments in a balanced
 fashion within a square block or field. The treatments are assigned
 randomly once in each row and column. The Latin square design
 included equal numbers of rows, columns, and treatments

Subjects	Treatment period 1	Treatment period 2	Treatment period 3	
Rat 1	VEH	UVI	Bexa	t1.2
Rat 2	Bexa	VEH	UVI	t1.3
Rat 3	UVI	Bexa	VEH	t1.4
Rat 4	VEH	UVI	Bexa	t1.5
Rat 5	Bexa	VEH	UVI	t1.6
Rat 6	UVI	Bexa	VEH	t1.7
Rat 7	VEH	UVI	Bexa	t1.8
Rat 8	Bexa	VEH	UVI	t1.9
				t1.10

210	across the EEG associated with low EMG signal. One observ-	Microdialysis surgeries	251
211	er blinded to the experimental codes of the animals scored the	Studies from our group have demonstrated reliable measure-	252
212	sleep data (Murillo-Rodríguez et al., 2019).	ments of monoamines (dopamine [DA], serotonin [5-HT],	253
213	Statistical analysis	norepinephrine [NE], and epinephrine [EP]) sampled from	254
214	All values are expressed as mean ± standard error of the mean.	nucleus accumbens (AcbC; Murillo-Rodríguez et al., 2017,	255
215	Statistical analyses were performed using StatView (version	2019). Therefore, we determined whether Bexa or UVI would	256
216	5.0.0, SAS Institute, USA). The significance of differences for	induce changes in the extracellular contents of monoamines	257
217	the experimental groups was determined using one-way anal-	collected by microdialysis means from AcbC and determined	258
218	ysis of variance (ANOVA) followed by Bonferroni test.	by analytical approaches. To achieve this goal, a new group of	259
219	$P < 0.05$ was considered statistically significant.	rats ($n = 6$) were anesthetized and mounted into the stereotaxic	260
220	Experiment 2: Sleep homeostasis under influence	frame (David Kopf Instruments, Tujunga, CA, USA) for im-	261
221	of Bexarotene or UVI 3003	plantation of a microdialysis guide cannula (IC guide;	262
222	Ethics approval, animals, chemicals and materials,	Bioanalytical Systems [BAS], West Lafayette, IN, USA) aimed	263
223	sleep-recording surgeries, and habituation processes	unilaterally into the AcbC (coordinates $A = +1.2$,	264
224	As described in Experiment 1 .	$L = +2.0$, and $H = -7.0$ mm, with reference to bregma	265
225	Sleep deprivation procedure	[Paxinos and Watson, 2005]). The microdialysis probe was	266
226	In addition to the characterization of the pharmacological ef-	attached onto the skull by dental cement. Once the surgery	267
227	fects of Bexa or UVI on the sleep-wake cycle, we tested	was completed, rats were placed into the microdialysis bowl	268
228	whether the RXR modulators would modify the sleep homeo-	(Ratum Microdialysis Stand-Alone System, MD-1404, BAS,	269
229	stasis. To achieve this goal, animals ($n = 8$) were subjected to	West Lafayette, IN, USA) during 7 days for post-surgery re-	270
230	total sleep deprivation (TSD) during 6 h by maintaining them	covery as well as habituation for the experimental conditions.	271
231	on continuous waking from 08:00 to 14:00 h. The sleep depri-	All surgical procedures of microdialysis surgery were accom-	272
232	vation procedure was developed by generating sounds (tap-	plished as previously reported (Murillo-Rodríguez et al.,	273
233	ping the cages) or by placing novel objects into the sleep	2017, 2019).	274
234	chambers (Murillo-Rodríguez et al., 2017). Upon the TSD	Microdialysis sampling procedures	275
235	was completed and under a blinded procedure, pharmacolog-	Once the recovery and habituation period of time was	276
236	ical challenges were administered to rats allowing them to	attained, rats were removed from the microdialysis bowls for	277
237	sleep ad libitum for the next 4 h (sleep rebound period). The	withdrawing the stylet from guide cannula. Next, the micro-	278
238	characterization and scoring the states of vigilance during the	dialysis probe (1 mm of length; polyacrylonitrile, MWCO =	279
239	sleep rebound period were carried out as previous criteria	30,000 Da; 340 µm OD; BAS, West Lafayette, IN, USA) was	280
240	(Murillo-Rodríguez et al., 2017). The sleep stages during the	inserted at 08:00 h. Then, artificial cerebrospinal fluid (aCSF	281
241	sleep rebound period were analyzed by one observer blinded	[composition: NaCl [147 mM], KCl [3 mM], CaCl ₂ [1.2 mM],	282
242	to the code of the rats.	MgCl ₂ [1.0 mM], pH 7.2]) was perfused through a miniature	283
243	Statistical analysis	tube (0.65 mm OD × 0.12 mm ID; BAS, West Lafayette, IN,	284
244	As described in Experiment 1 .	USA) attached to a 2.5-mL syringe (BAS, West Lafayette, IN,	285
245	Experiment 3: Neurochemical response to Bexarotene	USA) using a pump (flow rate 0.25 µL/min; BAS Bee, West	286
246	or UVI 3003	Lafayette, IN, USA). The probe was placed in the AcbC at	287
247	Ethics approval, animals, chemicals and materials,	least 24 h before the experiments in order to minimize the	288
248	habituation processes, and drugs preparation	damage made by the insertion and allow the probe's stabiliza-	289
249	and administrations	tion. The samples from stabilization period were excluded for	290
250	As described in Experiment 1 .	the final analyses. In addition, the probes in all microdialysis	291
		studies across our study were used < 5 days since previous	292
		studies have showed tissue damage, resulting in findings of	293
		gliosis at the implantation site between 3 and 7 days after	294
		implantation of microdialysis probe (Anderzhanova and	295
		Wotjak, 2013; Hammarlund-Udenaes, 2017; Murillo-	296
		Rodríguez et al., 2004). Twenty-four hours after the insertion	297
		of the probe, animals received the experimental trials, and	298
		samples were collected every 20 min at the beginning of each	299
		hour during the following 4 h. Later, all samples were stored	300

301	(− 80 °C; Revco Ultima PLUS, Thermo Scientific, Waltham, MA, USA) for further analysis. The microdialysis sampling procedure was developed as previously reported (Murillo-Rodríguez et al., 2017, 2019).		
302			
303			
304			
305	Measurements of monoamines using HPLC		
306	The collected microdialysis samples from treatments applied at either the lights-on or lights-off period were filtered (Millipore 0.22 μm; Merck Millipore, Darmstadt, Germany) and injected into high-performance liquid chromatography (HPLC; Modular Prominence, Shimadzu, Kyoto, Japan). The detection of DA, 5-HT, NE, and EP required a mobile phase of NaH ₂ PO ₄ (7 mM, pH 3.0), plus MEOH (3.5%), which was perfused into the HPLC at a flow rate of 80 μL/min (pump LC-20AT, Shimadzu, Kyoto, Japan). The separation of molecules was achieved by using a microbore column (octadecyl silica [3 μm, 100 × 1 mm], BAS, West Lafayette, IN, USA), under controlled temperature (22 °C; oven CTO-20A, Shimadzu, Kyoto, Japan). The detection of monoamines was obtained by an electrochemical detector (LC-4C; BAS, West Lafayette, IN, USA). The chromatographic data were stored on a personal computer (via computer controller CBM-20A, Shimadzu, Kyoto, Japan), and the concentrations of monoamines in analyzed samples were obtained by comparing the external known concentration of standards for DA, 5-HT, EP, and NE. The procedure for the measurements of monoamines was developed as described previously (Murillo-Rodríguez et al., 2017, 2019). The determination of contents of monoamines was achieved under a blinded procedure.		
307			
308			
309			
310			
311			
312			
313			
314			
315			
316			
317			
318			
319			
320			
321			
322			
323			
324			
325			
326			
327			
328			
329			
330	Statistical analysis		
331	The total value obtained for each molecule consisted in the sum of hourly collected samples from each neurotransmitter across 4 h post-treatments. Data from microdialysis experiments were represented as mean ± SEM, and the statistical differences among the experimental groups were determined by one-way ANOVA followed by Bonferroni's post hoc test. All statistical analyses were performed using the StatView software (version 5.0.0, SAS Institute, USA), and statistical differences among groups were determined if <i>P</i> < 0.05.		
332			
333			
334			
335			
336			
337			
338			
339			
340	Experiment 4: Bexarotene or UVI 3003 modulate adenosine contents		
341			
342	Ethics approval, animals, chemicals and materials, habituation processes, drugs preparation and administrations		
343			
344			
345	As described in Experiments 1 and 3.		
		Microdialysis surgeries	346
		Several pieces of evidence have suggested that adenosine (AD) is measurable from the basal forebrain (Kalinchuk et al., 2011; Sharma et al., 2017; Vazquez-DeRose et al., 2016). Then, in this part of our study, a new group of rats (<i>n</i> = 6) were anesthetized and mounted into the stereotaxic frame (David Kopf Instruments, Tujunga, CA, USA) for unilateral implantation of a microdialysis guide cannula (IC guide; Bioanalytical Systems [BAS], West Lafayette, IN, USA) aimed into the basal forebrain (<i>A</i> = − 0.35; <i>L</i> = 2.0; and <i>H</i> = − 7.5 mm, with reference to bregma [Paxinos and Watson, 2005]). All microdialysis surgery procedure was developed as described in Experiment 3 .	347 348 349 350 351 352 353 354 355 356 357 358
		Microdialysis sampling procedures	359
		As described in Experiment 3 .	360
		Analytical determination of adenosine	361
		As described in Experiment 3 , with the following differences, mobile phase was prepared with NaH ₂ PO ₄ (10 mM; pH 4.5) and MEOH (9%) perfused at a flow rate of 80 mL/min using a pump (LC-20AT, Prominence HPLC, Shimadzu, Japan). The detection of AD was achieved by using an UV detector (SPD-20A Prominence, Shimadzu, Kyoto, Japan) set to a wavelength of 254 nm (deuterium lamp). The HPLC procedure for detection of AD was developed as previously reported (Murillo-Rodríguez et al., 2017, 2019). To avoid interpretive bias, the dialysates were analyzed under a blinded code. For statistical analysis, the randomization code was then broken.	362 363 364 365 366 367 368 369 370 371 372
		Statistical analysis	373
		As described in Experiment 3 .	374
		Experiment 5: Acetylcholine contents after administration Bexarotene or UVI 3003	375 376
		Ethics approval, animals, chemicals and materials, habituation processes, drugs preparation and administrations, microdialysis surgeries	377 378 379
		As described in Experiments 1 and 4.	380
		Microdialysis sampling procedure	381
		As described in Experiment 4 with exception of aCSF which was composed by KCl (2.4 nM), Na ₂ SO ₄ (0.5 nM), NaCl (126.5 nM), CaCl ₂ (1.2 nM), NaHCO ₃ (27.5 nM), KH ₂ PO ₄ (0.5 nM), MgCl ₂ (0.8 nM), and dextrose (5.0 nM) at pH 6.8, the aCSF was perfused through a miniature tubing (0.65 mm	382 383 384 385 386

387 OD; 0.12 mm ID; BAS, West Lafayette, IN, USA) attached to
 388 a 2.5-mL syringe (BAS, West Lafayette, IN, USA) with a
 389 pump (flow rate 2 mL/min; BAS Bee, West Lafayette, IN,
 390 USA). All microdialysis procedures were developed as previ-
 391 ously reported (Murillo-Rodríguez et al., 2018).

392 **Acetylcholine measurement**

393 The HPLC settings for ACh detection was used as follows:
 394 C₁₂H₁₉BrN₂O₂ (100 nM) was added to the aCSF (Murillo-
 395 Rodríguez et al., 2018). In addition, an acetylcholine-choline
 396 assay kit (MF-8910; BAS, West Lafayette, IN, USA) was
 397 included for ACh detection. The separation of molecule was
 398 achieved by injecting samples into the HPLC at a flow rate of
 399 1 mL/min, under temperature of 28 °C (oven CTO-20A,
 400 Shimadzu, Kyoto, Japan), using a 10-cm analytical column
 401 (MF-6150, BAS, West Lafayette, IN, USA) and a mobile
 402 phase (Na₂HPO₄ [35 nM], EDTA [0.1 nM], and ProClin
 403 150 preservative (0.005%); BAS, West Lafayette, IN, USA)
 404 with pH 8.5. An electrochemical detector allowed the ACh
 405 determination (LC-4C; BAS, West Lafayette, IN, USA) main-
 406 taining the potential at +0.5 V. The procedure to determine
 407 ACh was developed as previously reported (Grupe et al.,
 408 2013; Murillo-Rodríguez et al., 2018). A blinded analysis
 409 strategy was used to minimize the possibility of bias in exper-
 410 imental results.

411 **Relative recovery of the microdialysis probes**

412 The in vitro relative recovery experiments in all microdialysis
 413 studies (monoamines, AD, and ACh sampling) were achieved
 414 by inserting the microdialysis probes into a solution contain-
 415 ing external known standards of tested molecules (DA, 5-HT,
 416 NE, EP, AD, and ACh) under similar conditions as
 417 Experiments 3–5 were developed. The dialysates were collect-
 418 ed in a triplicate and each sample was analyzed. Then, the
 419 peak area ratio for monoamines, AD, or ACh was calculated
 420 against the external known standards. The relative recovery
 421 data were calculated as follows: Recovery rate (%) D (the
 422 peak area ratio of the dialysate) / (the peak area ratio of the
 423 dialysate in the test solution). The in vitro relative recovery
 424 procedure was developed as previously reported (Huang et al.,
 425 2013; Kho et al., 2017; Kou et al., 2019; Murillo-Rodríguez
 426 et al., 2004; Porkka-Heiskanen et al., 2000).

427 **Histological verification of microdialysis probes implantation**

428 The placement of microdialysis probes into target areas was
 429 verified as described previously (Blanco-Centurion et al.
 430 2006). Briefly, after the microdialysis study, rats were
 431 sacrificed by a lethal dose of pentobarbital for the standard
 432 procedure of vascular perfusion (saline solution [0.9%]
 433 followed by formaldehyde [4%]). The brain was collected

and post-fixed overnight in formaldehyde (4%) followed by 434
 10, 20, and 30% sucrose/0.1 M PBS during 24 h/each con- 435
 centration. Later, brains were cut in coronal sections (20 µm) 436
 using a Portable Bench-top Cryostat (Leica CM1100, Wetzlar, 437
 Germany) and collected in 1:5 serial order. For verification of 438
 probe location, one series was used for plotting the targeted 439
 brain area (Paxinos and Watson, 2005). Sections that showed 440
 the microdialysis probe localization outside of target area were 441
 excluded for the final neurochemical analysis. The histologi- 442
 cal procedures were developed as previously reported 443
 (Blanco-Centurion et al. 2006; Murillo-Rodríguez et al., 444
 2004). 445

Statistical analysis 446

As described in Experiment 3. 447

**Experiment 6: Bexarotene or UVI 3003 affects c-Fos 448
 expression in hypothalamus** 449

**Ethics approval, animals, chemicals and materials, 450
 habituation processes, and drugs preparation 451
 and administrations** 452

As described in Experiment 1. 453

Immunohistochemical studies 454

The expression of *c-Fos* by individual neurons normally is 455
 used as a marker of cell activation allowing to elucidate a 456
 functional neuroanatomical mapping in response to specific 457
 stimuli (Perrin-Terrin et al., 2016). Thus, to characterize the 458
 effects of Bexa or UVI on molecular activity in a brain area 459
 related to the sleep-wake cycle control, such as the hypothal- 460
 amus, we analyzed the *c-Fos* expression in such region. This 461
 brain area was selected since it has been suggested as a key 462
 element in the modulation of the sleep-wake cycle (Arrigoni 463
 et al., 2019; Jones, 2019). Then, a new set of animals (*n* = 24) 464
 were used for the *c-Fos* studies. One group of rats received at 465
 09:00 h a systemic (i.p.) injection of either control (*n* = 4), 466
 Bexa (*n* = 4), or UVI (*n* = 4), and 1 h later, they were sacrificed 467
 by a lethal dose of pentobarbital for the standard procedure of 468
 vascular perfusion. Same experimental condition was carried 469
 out at lights-off period: At 21:00 h, animals were sacrificed 1 h 470
 later after receiving an application of control (*n* = 4), Bexa 471
 (*n* = 4) or UVI (*n* = 4). Brains were collected and processed 472
 for *c-Fos* immunostaining. The identification of the hypothal- 473
 amus included slides collected from coordinates -0.12 to - 474
 3.48 mm (from bregma according to the Rat Brain Atlas 475
 [Paxinos and Watson, 2005]). The Fos staining was developed 476
 as follows: we used standardized procedures for 477
 immunohistochemically detection of *c-Fos* by conventional 478
 avidin-biotin-immunoperoxidase chemicals to localize an 479

480	antiserum raised against a synthetic N-terminal fragment of	531
481	human Fos protein (de-la-Cruz et al., 2018). The selected sec-	532
482	tions were washed 3 times in PBS (0.1 M, pH 7.3) and incu-	533
483	bated with the endogenous peroxidase (0.28% for 1 min) at	534
484	room temperature and with H ₂ O ₂ (3%) and MEOH (10%) in	535
485	PBS (0.1 M) for 20 min at room temperature. Later, slides	536
486	were washed 3 times in PBS (0.1 M, pH 7.3) and blocked	537
487	with 10% donkey or goat serum diluted in PBS (containing	
488	0.2% Triton X-100; Sigma-Aldrich, St Louis, MO, USA).	
489	Subsequently, the sections were incubated overnight with the	
490	corresponding primary antibody at 4 °C (goat anti-c-fos	
491	1:100; Santa Cruz Biotechnology, Inc., Dallas, TX, USA).	
492	On the next day, slides were again washed 3 times in PBS	
493	(0.1 M, pH 7.3) and incubated for 2 h at room temperature	
494	with the respective biotinylated secondary antibody (1:250,	
495	goat anti-mouse IgG, 125 K6063; Sigma-Aldrich, St Louis,	
496	MO, USA; donkey anti-rabbit IgG; Vector Laboratories,	
497	Burlingame, CA, USA). Next, the sections were washed other	
498	3 times in PBS (0.1 M, pH 7.3) and incubated with the per-	
499	oxidase complex (1:2000; Sigma-Aldrich, St. Louis, MO,	
500	USA) for 1 h in the dark. Lastly, following 3 washes in	
501	PBS, immunolabeling was revealed by exposing the slides	
502	to 0.05% diaminobenzidine (Sigma-Aldrich, St Louis, MO,	
503	USA) and H ₂ O ₂ (0.03%) in PBS. The reaction was stopped	
504	using PBS and sections were then washed several times again	
505	in PBS. The sections were mounted onto chrome alum	
506	gelatin-coated slides, dehydrated through graded alcohols,	
507	cleared in xylene, and cover slipped using DPX Mountant	
508	(Sigma-Aldrich, St Louis, MO, USA). The reproducibility of	
509	the c-Fos protocol was confirmed by repeating the whole pro-	
510	cedure with additional series that contained approximately the	
511	same number of sections from all experimental groups using	
512	the same primary antibody. The whole c-Fos procedure was	
513	developed as previously reported (de-la-Cruz et al., 2018). To	
514	minimize bias, experimenters were not aware of the identity of	
515	the treatments in the immunohistochemical analysis.	
516	The expression pattern of c-Fos in response to Bexarotene	
517	or UVI 3003	
518	A similar number of sections of the hypothalamus (coordi-	
519	nates from -0.12 to -3.48 mm, according to the Rat Brain	
520	Atlas [Paxinos and Watson, 2005]) of both hemispheres of	
521	each rat, from all experimental groups, were included in the	
522	counting for c-Fos staining. Bright field images were	
523	photographed with a digital camera (AxioCam ICc1; Carl	
524	Zeiss Microscopy, Oberkochen, Germany) on a microscope	
525	(× 100 objective lens; Zeiss Imager A.2. Carl Zeiss	
526	Microscopy, Oberkochen, Germany) with the image analysis	
Q1527	computer software (ZEN 2012, Blue Edition, Carl Zeiss	
528	Microscopy, Oberkochen, Germany). The analysis of images	
529	included c-Fos immunohistochemical patterns from slides	
530	containing the hypothalamus. We counted in 3 consecutive	
	sections (coordinates -0.12 to -3.48 mm; from bregma ac-	531
	cording to the Rat Brain Atlas [Paxinos and Watson, 2005]) to	532
	perform these analyses in 4 animals per group. To minimize	533
	experimental bias, the tally of c-Fos expression was developed	534
	under a blind code, meaning that experimenters were unaware	535
	of the identity of treatments. The whole c-Fos study was car-	536
	ried out as described previously (de-la-Cruz et al., 2018).	537
	Statistical analysis	538
	As described in Experiment 1 .	539
	Experiment 7: Characterization of neurons expressing	540
	neuronal nuclear protein (NeuN) in hypothalamus	541
	after the application of Bexarotene or UVI 3003	542
	Ethics approval, animals, chemicals and materials,	543
	habituation processes, and drugs preparation	544
	and administrations	545
	As described in Experiment 1 .	546
	Immunohistochemical studies	547
	Several studies have reported the activity of NeuN as a reliable	548
	marker of postmitotic neurons as well as neuronal differentia-	549
	tion (Duan et al., 2016; Gusel'nikova and Korzhevskiy,	550
	2015). Having this in mind, we characterized whether admin-	551
	istrations of Bexa or UVI might exert effects on NeuN expres-	552
	sion in hypothalamus. To achieve this aim, standardized pro-	553
	protocols for immunohistochemically detection of NeuN were	554
	used (de-la-Cruz et al., 2018; Hight et al., 2010). In detail,	555
	sections containing the hypothalamus were washed 3 times	556
	in PBS (0.1 M, pH 7.3) and blocked with 10% donkey or goat	557
	serum diluted in PBS (containing 0.2% Triton X-100).	558
	Subsequently, sections were incubated overnight with the cor-	559
	responding primary antibody at 4 °C (mouse anti-NeuN;	560
	1:500; Millipore, Billerica, MA, USA). On the next day, the	561
	sections were washed 3 times in PBS (0.1 M, pH 7.3) and	562
	incubated for 2 h at room temperature with the respective	563
	biotinylated secondary antibody (1:250; goat anti-mouse	564
	IgG, 125 K6063; Sigma, donkey anti-rabbit IgG; Vector	565
	Laboratories, Burlingame, CA, USA). Next, the sections were	566
	washed 3 times in PBS (0.1 M, pH 7.3) and incubated with the	567
	peroxidase complex (1:2000, Sigma-Aldrich, St Louis, MO,	568
	USA) for 1 h in the dark. Lastly, following 3 washes in PBS,	569
	sections were exposed for revelation to 0.05% diaminobenzi-	570
	dine (Sigma-Aldrich, St Louis, MO, USA) and 0.03% H ₂ O ₂	571
	in PBS. The NeuN immunohistochemical studies were devel-	572
	oped as previously reported (de-la-Cruz et al., 2018).	573

574 **The counting number of neurons expressing NeuN**

575 As described in [Experiment 6](#).

576 **Statistical analysis**

577 As described in [Experiment 1](#).

578 **Results**

579 **Bexarotene and UVI-3003 control the sleep-wake**
580 **cycle**

Q1581 To determine the effect of RXR on sleep, Bexa or UVI was
582 systemically (i.p.) administered and sleep-wake cycle was re-
Q1583 corded and analyzed. As shown in Fig. 1 (panel a), application

Subjects	Treatment Period 1	Treatment Period 2	Treatment Period 3
Rat 1	VEH	UVI	Bexa
Rat 2	Bexa	VEH	UVI
Rat 3	UVI	Bexa	VEH
Rat 4	VEH	UVI	Bexa
Rat 5	Bexa	VEH	UVI
Rat 6	UVI	Bexa	VEH
Rat 7	VEH	UVI	Bexa
Rat 8	Bexa	VEH	UVI

Q16 **Fig. 1** Effects of total time (4 h) of wakefulness (W), slow-wave sleep (SWS), and rapid eye movement sleep (REMS) after the administration (i.p.) at the beginning of either the lights-on (panel a) or lights-off period (panel b) of vehicle, bexarotene (Bexa), or UVI 3003 (UVI; 1 mM each compound). Application of Bexa at the beginning of the lights-on period increased W ($P < 0.0001$), decreased SWS ($P < 0.0001$), and caused no changes in REMS ($P = 0.3$; panel a) whereas UVI caused opposite effects in W and SWS (panel a). Bonferroni test showed significant differences in W and SWS between VEH vs. Bexa ($P < 0.0001$) and Bexa vs. UVI ($P < 0.0001$). On the contrary, Bexa injected at the beginning of the lights-off period (panel b) decreased W ($P < 0.0002$) and enhanced SWS ($P < 0.0006$) whereas REMS remained with no changes ($P = 0.5$). In addition, UVI exerted no significant changes if injected at the dark period in W, SWS, or REMS. Bonferroni test showed differences in W and SWS among VEH vs. Bexa ($P < 0.0001$) and Bexa vs. UVI ($P < 0.0001$; *vs. control; #vs. Bexa)

of Bexa at the beginning of the lights-on period enhanced W (584 $F_{(2, 21)} = 72.113, P < 0.0001$) and decreased SWS ($F_{(2, 21)} =$ 585 $68.356, P < 0.0001$) while REMS was found with no statisti- 586 cal changes ($F_{(2, 21)} = 1.009, P = 0.3$). When UVI was injected 587 at the beginning of the lights-on period, no significant differ- 588 ences were seen in W, SWS, or REMS (Fig. 1, panel a). 589 Bonferroni test showed significant differences in alertness 590 and SWS between VEH vs. Bexa ($P < 0.0001$) and Bexa vs. 591 UVI ($P < 0.0001$). 592

Next, we assessed the effect of Bexa or UVI on the sleep- 593 wake cycle if injected at the beginning of the dark period (Fig. 594 1, panel b). The results showed that application of Bexa de- 595 creased W ($F_{(2, 21)} = 12.863, P < 0.0002$) and enhanced SWS 596 ($F_{(2, 21)} = 10.779, P < 0.0006$) whereas REMS remained with 597 no changes ($F_{(2, 21)} = 0.535, P = 0.5$). In addition, UVI-treated 598 animals showed no statistical differences in W, SWS, or 599 REMS. Further disparities addressed by Bonferroni test 600 showed significant differences in W and SWS among VEH 601 vs. Bexa ($P < 0.0001$) and Bexa vs. UVI ($P < 0.0001$). We 602 conclude that RXR modulates sleep in a time-dependent 603 fashion. 604

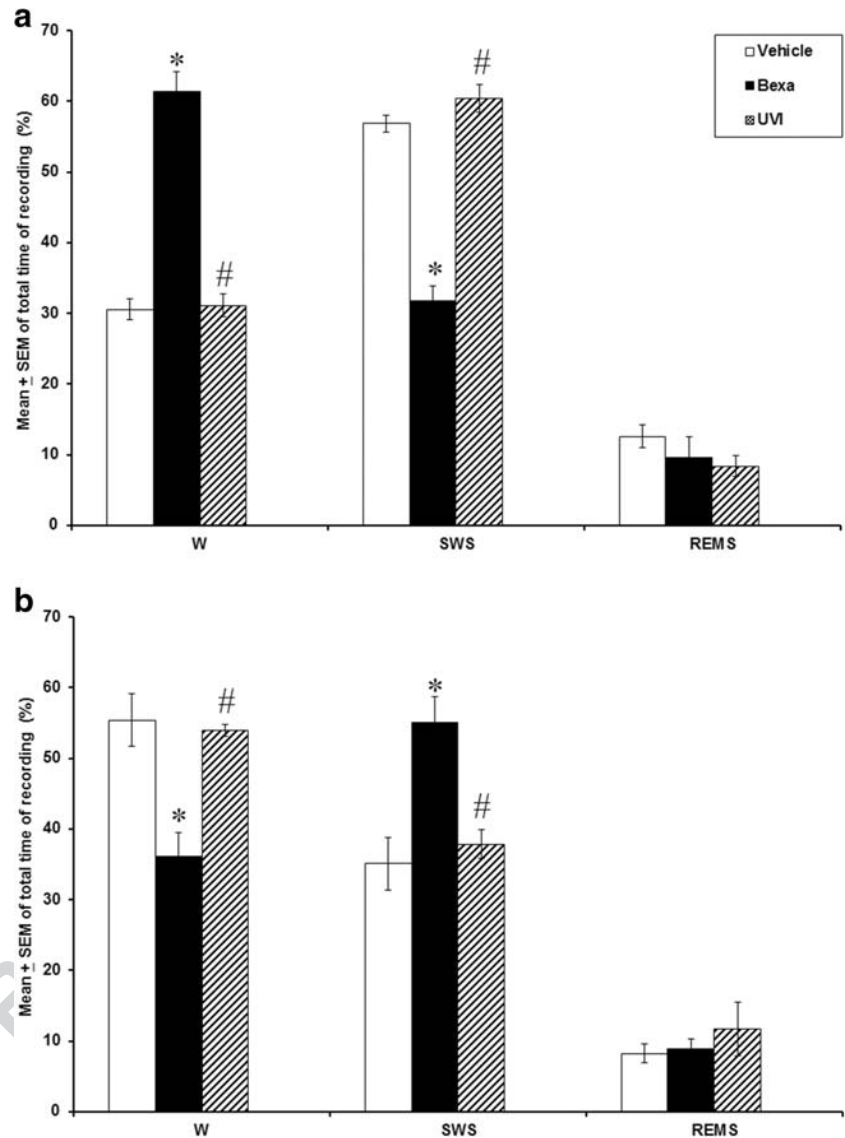
Sleep homeostasis is affected by application 605 of bexarotene or UVI-3003 606

In addition to the effects on sleep during the lights-on or 607 lights-off period, RXR caused marked changes in sleep ho- 608 meostasis (Fig. 2). Six hours after TSD, rats received an intra- 609 peritoneal injection of either Bexa or UVI and sleep rebound 610 was analyzed. The application of the RXR agonist increased 611 the W amount during the sleep rebound ($F_{(2, 21)} = 52.59,$ 612 $P < 0.0001$) and no changes were observed in SWS ($F_{(2, 21)} =$ 613 $15.345, P < 0.001$) while decreased REMS ($F_{(2, 21)} =$ 614 $14.028, P < 0.0001$). Moreover, UVI did not modify the W 615 amount but enhanced the SWS amount and decreased 616 REMS. Bonferroni post hoc test showed significant differ- 617 ences in W (VEH vs. Bexa, $P < 0.0001$; Bexa vs. UVI, 618 $P < 0.0001$), SWS (VEH vs. UVI, $P < 0.0001$; Bexa vs. 619 UVI, $P < 0.0003$), and REMS (VEH vs. Bexa, $P < 0.04$; 620 VEH vs. UVI, $P < 0.0001$; Bexa vs. UVI, $P < 0.005$). These 621 findings suggest that RXR modulates the sleep homeostasis 622 elicited by the sleep rebound after a TSD. 623

Neurochemical analysis of DA, 5-HT, NE, EP, AD, 624 and ACh contents in response to bexarotene or UVI 625 3003 626

Systemic administration of Bexa or UVI modified the sleep- 627 wake cycle, suggesting that the RXR might be involved in the 628 modulation of the states of vigilance via the release of neuro- 629 chemicals related to the sleep control. In support of this as- 630 sumption, the technique of microdialysis was coupled for 631 sampling molecules related to the sleep-wake cycle control 632

Fig. 2 Effects on total time (4 h) of wakefulness (W), slow-wave sleep (SWS), and rapid eye movement sleep (REMS) after 6 h of total sleep deprivation in rats that received a systemic application (i.p.) or either vehicle, bexarotene (Bexa), or UVI 3003 (UVI; 1 mM each compound). During the sleep rebound period, Bexa-treated animals showed an enhancement in W ($P < 0.0001$) with no changes in SWS ($P < 0.001$) whereas REMS was decreased ($P < 0.0001$). UVI induced opposite effects in the sleep rebound period in SWS and REMS. Bonferroni test showed differences in W (VEH vs. Bexa, $P < 0.0001$; Bexa vs. UVI, $P < 0.0001$), SWS (VEH vs. UVI, $P < 0.0001$; Bexa vs. UVI, $P < 0.0003$), and REMS (VEH vs. Bexa, $P < 0.04$; VEH vs. UVI, $P < 0.0001$; Bexa vs. UVI, $P < 0.005$; *vs. control; #vs. Bexa)



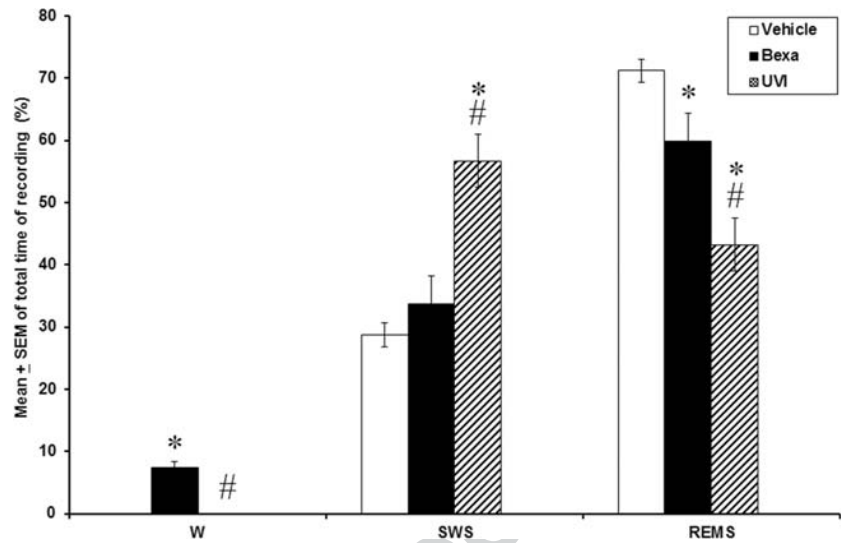
633 under the likely influence of Bexa or UVI. The total amount of
 634 the extracellular levels of DA, 5-HT, NE, EP, AD, and ACh
 635 was determined by the highly sensitive analytical technique
 636 HPLC which enables the quantification of low concentrations
 637 in small size samples (Hammarlund-Udenaes, 2017). The
 638 schematic illustration of the position of the probe into AcbC
 639 or basal forebrain is shown in Fig. 3 (panels a or b,
 640 respectively).

641 Next, we tested the ability of Bexa or UVI to modify the
 642 extracellular levels of DA, 5-HT, NE, EP, AD, and ACh.
 643 When challenged with Bexa at the start of the lights-on cycle,
 644 we found an increase in DA ($F_{(2, 21)} = 304.273$, $P < 0.0001$;
 645 Fig. 4, panel a), 5-HT ($F_{(2, 21)} = 69.859$, $P < 0.0001$; Fig. 4,
 646 panel b), but no significant changes were found in NE ($F_{(2, 21)} = 0.517$, $P = 0.6$; Fig. 4, panel c) but an increase was found
 647 in EP ($F_{(2, 21)} = 9.442$, $P < 0.001$; Fig. 4, panel d), AD ($F_{(2, 21)} = 174.966$, $P < 0.0001$; Fig. 4, panel e), and ACh ($F_{(2, 21)} =$

30.588, $P < 0.0001$; Fig. 4, panel f). Opposite results were
 650 found in UVI-treated rats in the sampled neurochemicals
 651 (Fig. 4, panels a–f). Further post hoc analysis via Bonferroni
 652 test showed significant differences among treatments for DA
 653 (VEH vs. Bexa, $P < 0.0001$; Bexa vs. UVI, $P < 0.0001$), 5-HT
 654 (VEH vs. Bexa, $P < 0.0001$; Bexa vs. UVI, $P < 0.0001$), EP
 655 (VEH vs. Bexa, $P < 0.0005$; Bexa vs. UVI, $P < 0.003$), AD
 656 (VEH vs. Bexa, $P < 0.0001$; Bexa vs. UVI, $P < 0.0001$), and
 657 ACh (VEH vs. UVI, $P < 0.0001$; Bexa vs. UVI, $P < 0.0001$).
 658 The data suggest that RXR modulates the extracellular levels
 659 of neurochemicals linked to the sleep control if injected at the
 660 lights-on period.
 661

662 Next, we analyzed if molecules related to the sleep modulation
 663 might be under the influence of RXR during the dark phase.
 664 To achieve this aim, Bexa or UVI was injected 1 h after
 665 the beginning of the lights-off period, and dialysates were
 666 collected across 4 h. This treatment regimen was highly

Fig. 3 Position of the microdialysis probe into the nucleus accumbens (AcbC) or basal forebrain. The schematic illustration from the rat brain atlas (Paxinos and Watson, 2005) shows the location of the microdialysis probe into the AcbC (coordinates $A = +1.2$, $L = +2.0$, and $H = -7.0$ mm; panel a) or into the basal forebrain (coordinates $A = -0.35$; $L = 2.0$; and $H = -7.5$ mm; panel b). AcbC, nucleus accumbens; LPO, lateral preoptic area. Scale bar 100 mm



667 effective for decreasing the contents of DA in Bexa-treated
 668 rats ($F_{(2, 21)} = 37.643$, $P < 0.0001$; Fig. 5, panel a), but en-
 669 hanced 5-HT ($F_{(2, 21)} = 7.481$, $P < 0.003$; Fig. 5, panel b),
 670 and no significant changes were found for NE ($F_{(2, 21)} =$
 671 2.749 , $P > 0.08$; Fig. 5, panel c) and EP ($F_{(2, 21)} = 1.049$,
 672 $P = 0.3$; Fig. 5, panel d). Moreover, Bexa decreased AD
 673 ($F_{(2, 21)} = 257.340$, $P < 0.0001$; Fig. 5, panel e) and ACh
 674 contents ($F_{(2, 21)} = 380.604$, $P < 0.0001$; Fig. 5, panel f).
 675 Remarkably, UVI induced opposite effects in DA, 5-HT,
 676 AD, and ACh measurements (Fig. 5, panels a, b, e, and f,
 677 respectively). Further multiple comparisons by Bonferroni test
 678 showed significant differences among the experimental trials
 679 for DA (VEH vs. Bexa, $P < 0.0001$; Bexa vs. UVI,
 680 $P < 0.0001$), 5-HT (VEH vs. Bexa, $P < 0.001$; Bexa vs. UVI,
 681 $P < 0.009$), AD (VEH vs. Bexa, $P < 0.0001$; Bexa vs. UVI,
 682 $P < 0.0001$), and ACh (VEH vs. UVI, $P < 0.0001$; Bexa vs.
 683 UVI, $P < 0.0001$). The microdialysis data (lights-on/lights-off
 684 period) suggest that RXR seems to modulate the extracellular
 685 levels of neurochemicals related to the sleep-wake cycle con-
 686 trol in a time-dependent fashion.

687 **c-Fos immunohistochemistry in the hypothalamus**
 688 **after administration of Bexarotene or UVI 3003**

689 Because *c-Fos* has been used under different experimental
 690 paradigms as a functional marker of neuronal activity after
 691 diverse stimuli (Gallo et al., 2018; Jaworski et al., 2018;
 692 Kovács, 2008), in a subsequent experiment, we tested whether
 693 RXR might induce *c-Fos* expression in hypothalamus, a brain
 694 region linked to sleep modulation (Arrigoni et al., 2019;
 695 Jones, 2019). The schematic representations of rat brain sec-
 696 tions at rostral-caudal planes used for the immunohistochemi-
 697 cal study (according to the Rat Brain Atlas [Paxinos and
 698 Watson, 2005]) are shown in Fig. 6 (panel a). Compared with
 699 respective control (Fig. 6, panel b), Bexa applied at the

beginning of the lights-on period enhanced *c-Fos* activity 700
 (Fig. 6, panel c) whereas UVI exerted opposite results (Fig. 701
 6, panel c). In contrast to observed in the lights-on period, and 702
 compared with respective control (Fig. 6, panel e), the admin- 703
 istration of RXR agonist at 1 h after the start of the dark phase 704
 did not induce difference in *c-Fos* immunorexpression in hy- 705
 pothalamus (Fig. 6, panel f). Similar results were observed in 706
 UVI-treated rats (Fig. 6, panel g). Next, we determined wheth- 707
 er this pattern would be statistically different among experi- 708
 mental treatments, then the number of *c-Fos* expression in 709
 hypothalamus from VEH, Bexa, and UVI groups was counted. 710
 When treatments were applied at the beginning of the 711
 lights-on period, and as compared with respective control, 712
 Bexa increased the pattern expression of *c-Fos* in the hypo- 713
 thalamus while UVI induced an opposite effect ($F_{(2, 9)} =$ 714
 18.302, $P < 0.0007$; Fig. 6, panel h). Bonferroni test showed 715
 significant differences among experimental groups (VEH vs. 716
 Bexa, $P < 0.004$; VEH vs. UVI, $P < 0.05$; Bexa vs. UVI, 717
 $P < 0.0002$). Unlike the lights-on period, there were no signif- 718
 icant differences in the number of positive *c-Fos* immunore- 719
 activity in the dark phase after the pharmacological treatments 720
 ($F_{(2, 9)} = 0.510$, $P = 0.6$; Fig. 6, panel i). We conclude that *c-* 721
Fos expression in hypothalamus reacted in a photoperiod- 722
 dependent fashion in the presence of RXR agonist/antagonist. 723

724 **Characterization of neurons expressing NeuN**
 725 **in hypothalamus after the application of bexarotene**
 726 **or UVI 3003**

727 We assessed the impact of Bexa or UVI on the expression of
 728 NeuN in hypothalamus. Compared with the control group
 (Fig. 7, panel a), Bexa-treated animals showed higher NeuN
 729 expression (Fig. 7, panel b) whereas UVI caused a discrete
 730 activity of this neuronal marker (Fig. 7, panel c) when treat-
 731 ments were given at the beginning of the lights-on period. 732
 733

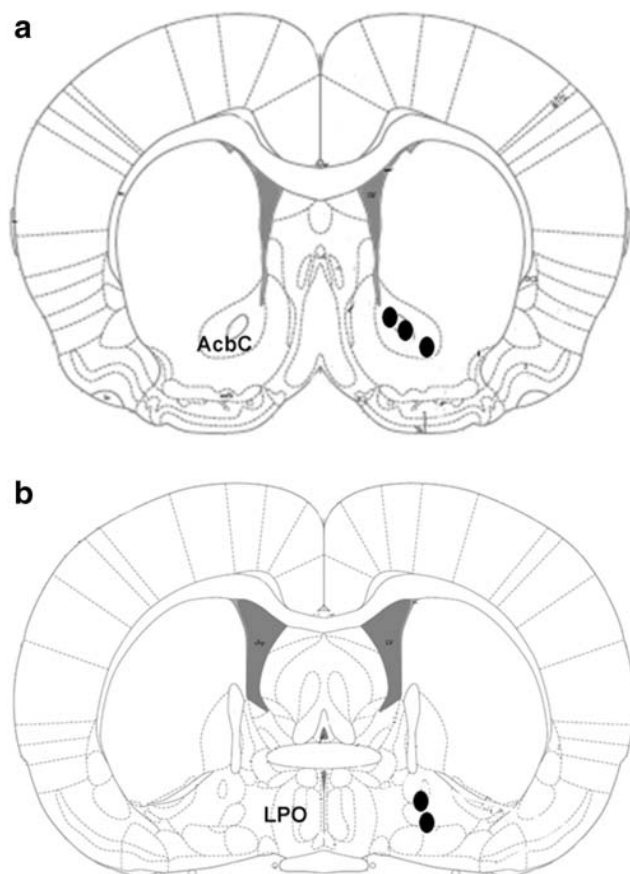


Fig. 4 Extracellular levels of dopamine (DA), serotonin (5-HT), norepinephrine (NE), epinephrine (EP), adenosine (AD), and acetylcholine (ACh) collected from either the AcbC or basal forebrain after treatment (i.p.) of either bexarotene (Bexa) or UVI 3003 (UVI; 1 mM each compound) during the lights-on period. When challenged with Bexa given at the beginning of the lights-on period, DA ($P < 0.0001$; panel a) and 5-HT ($P < 0.0001$; panel b) were enhanced and no significant changes were found in NE ($P = 0.6$; panel c). However, NE increased EP ($P < 0.001$; panel d), as well as AD ($P < 0.0001$; panel e) and ACh ($P < 0.0001$; panel f). UVI caused opposite effects in the levels of the neurochemicals. Bonferroni test showed differences for DA (VEH vs. Bexa, $P < 0.0001$; Bexa vs. UVI, $P < 0.0001$), 5-HT (VEH vs. Bexa, $P < 0.0001$; Bexa vs. UVI, $P < 0.0001$), EP (VEH vs. Bexa, $P < 0.0005$; Bexa vs. UVI, $P < 0.003$), AD (VEH vs. Bexa, $P < 0.0001$; Bexa vs. UVI, $P < 0.0001$), and ACh (VEH vs. UVI, $P < 0.0001$; Bexa vs. UVI, $P < 0.0001$; *vs. control; #vs. Bexa)

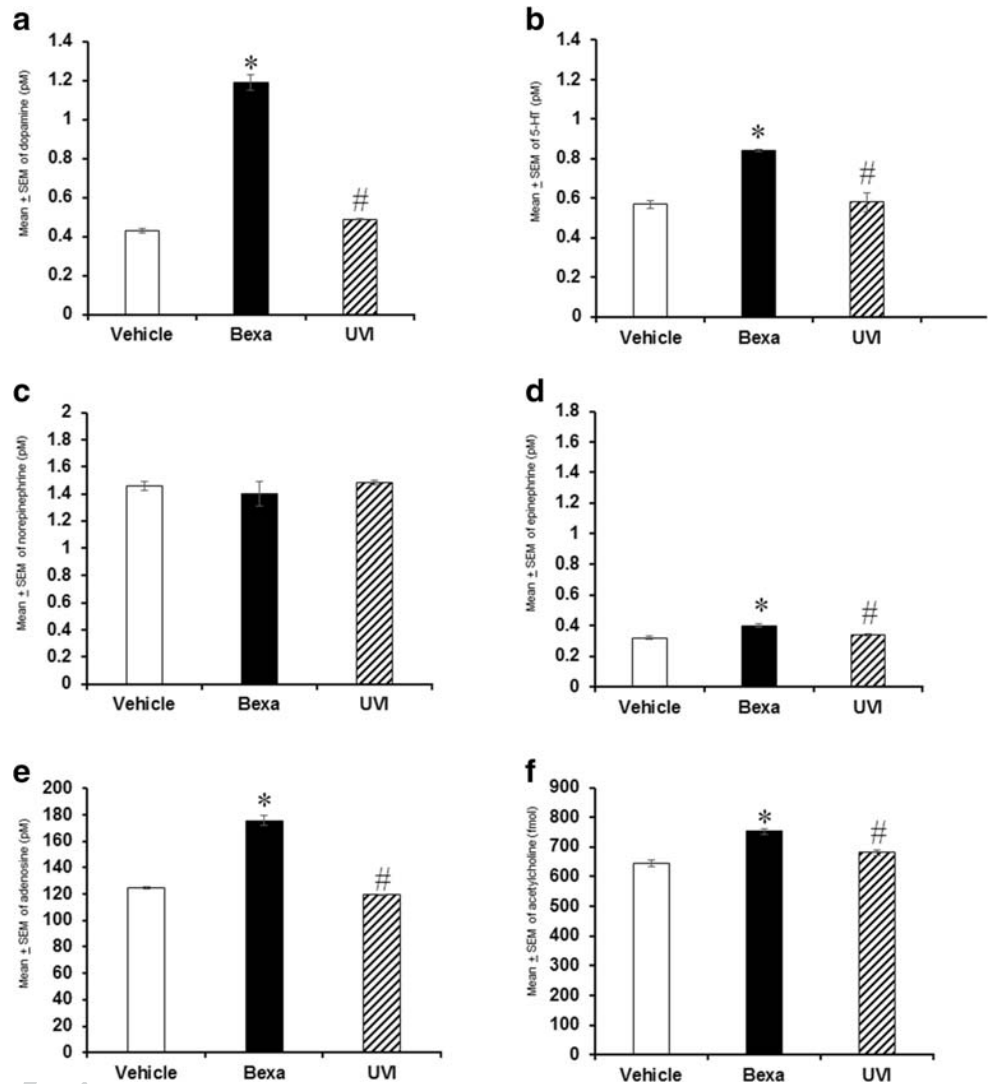
(VEH vs. Bexa, $P < 0.0001$; VEH vs. UVI, $P < 0.0001$; Bexa vs. UVI, $P < 0.0001$). Remarkably, when treatments were applied at the lights-off period, NeuN expression was decreased in Bexa-treated rats whereas UVI caused an opposite result ($F_{(2, 9)} = 214.310$, $P < 0.0001$; Fig. 7, panel h). Bonferroni test showed significant differences among experimental groups (VEH vs. Bexa, $P < 0.0001$; VEH vs. UVI, $P < 0.0001$; Bexa vs. UVI, $P < 0.0001$). These interesting results suggest that NeuN expression in hypothalamus after Bexa or UVI treatments showed a time-dependent effect.

Discussion

The present study provides the first detailed description of the pharmacological impact exerted by RXR agonist or antagonist in the sleep-wake cycle. Previous studies using bexarotene (Bexa) or UVI 3003 (UVI) have demonstrated their neurophysiological activity (Dheer et al., 2019; He et al., 2018; Martin et al., 2019; Simandi et al., 2018; Tu et al., 2018; Tunctan et al., 2018; Zhang et al., 2019), including a wider spectrum of positive outcomes, including glaucoma, cognitive, or motor improvements in animal models useful for the study of Alzheimer's and Parkinson's disease (Casali et al., 2018; McFarland et al., 2013; Simandi et al., 2018; Yu et al., 2015). However, in these studies, the role of retinoid X receptor (RXR) in sleep modulation was never described, and the role of this nuclear receptor in controlling the sleep-wake cycle and related neurochemicals remained therefore unclear. Here, we administered Bexa or UVI at either the beginning of the lights-on or the lights-off period, and sleep ad libitum, sleep homeostasis, extracellular levels of dopamine (DA), serotonin (5-HT), norepinephrine (NE), epinephrine (EP), adenosine (AD), and acetylcholine (ACh) collected from either the AcbC or basal forebrain were analyzed. In addition, *c-Fos* and NeuN expression in the hypothalamus was characterized in treated rats when compounds were given at the start of the lights-on or lights-off period. Our results showed that when given at the beginning of the lights-on period, Bexa increased wakefulness (W), decreased slow-wave sleep (SWS), and caused no changes in rapid eye movement sleep (REMS) whereas UVI caused opposite effects. On the other hand, when Bexa was injected at the start of the lights-off period, alertness was decreased and SWS was enhanced whereas REMS remained with no changes. Complementarily, UVI showed no significant changes in the states of vigilance if administered at the beginning of the lights-off period. In addition, when sleep homeostasis was analyzed in response to the compounds, we found that during the sleep rebound period after total sleep deprivation, Bexa enhanced W but induced no changes in SWS while REMS was decreased. Interestingly, UVI induced contrary effects in the sleep rebound period.

When experimental challenges were applied at the start of the dark period, and compared with the respective control group (Fig. 7, panel d), we found that Bexa decreased the immunoreactivity to NeuN (Fig. 7, panel e) whereas UVI induced a higher expression of this neuronal marker (Fig. 7, panel f). Statistical analysis of number of NeuN-positive neurons showed that Bexa enhanced this neuronal marker whereas UVI decreased the immunoreactivity to NeuN when treatments were given at the start of the lights-on period ($F_{(2, 9)} = 130.614$, $P < 0.0001$; Fig. 7, panel g) Bonferroni test showed significant differences among experimental groups

Fig. 5 Extracellular contents of dopamine (DA), serotonin (5-HT), norepinephrine (NE), epinephrine (EP), adenosine (AD), and acetylcholine (ACh) collected from either the AcbC or basal forebrain after application (i.p.) of either bexarotene (Bexa) or UVI 3003 (UVI; 1 mM each compound) during the lights-off period. Bexa decreased the contents of DA ($P < 0.0001$; panel a) but enhanced 5-HT ($P < 0.003$; panel b), and no significant differences were found in NE ($P = 0.3$; panel c) or EP ($P = 0.08$; panel d). However, Bexa decreased AD ($P < 0.0001$; panel e) and ACh ($P < 0.0001$; panel f). UVI induced opposite effects in the analyzed neurochemicals. Further multiple-comparison correction by Bonferroni test showed differences in DA (VEH vs. Bexa, $P < 0.0001$; Bexa vs. UVI, $P < 0.0001$), 5-HT (VEH vs. Bexa, $P < 0.001$; Bexa vs. UVI, $P < 0.009$), AD (VEH vs. Bexa, $P < 0.0001$; Bexa vs. UVI, $P < 0.0001$), and ACh (VEH vs. UVI, $P < 0.0001$; Bexa vs. UVI, $P < 0.0001$); *vs. control; #vs. Bexa)



793 In regard to the neurochemical studies, when Bexa was
 794 given at the beginning of the lights-on period, we observed
 795 an increase in DA and 5-HT contents whereas no significant
 796 changes were found in NE. However, NE, AD, and ACh
 797 levels were increased in Bexa-treated animals. In addition,
 798 the UVI administration caused opposite effects in the extra-
 799 cellular levels of the neurochemicals analyzed. Remarkably,
 800 injection of Bexa during the lights-off period decreased the
 801 contents of DA but increased 5-HT while no significant dif-
 802 ferences were observed in NE or EP while a decrease for AD
 803 and ACh was observed. By contrast, UVI induced opposite
 804 effects in the extracellular levels of DA, 5-HT, AD, and ACh
 805 as determined using HPLC means.

806 The results from the immunohistochemical experiment
 807 showed that Bexa enhanced *c-Fos* expression in hypothala-
 808 mus while a contrary profile was found in UVI-treated rats
 809 when compounds were applied at the beginning of the lights-
 810 on period. Interestingly, no differences were found in *c-Fos*
 811 expression in hypothalamus in Bexa-treated rats as well as in

animals that received UVI if drugs were given at the start of
 the lights-off period. Our findings indicate for the first time
 that RXR modifies the neuronal activity in hypothalamus as
 determined by *c-Fos* immunohistochemical approaches. In
 complementary study, we investigated whether RXR might
 modulate NeuN expression in hypothalamus of animals that
 received a systemic application of either Bexa or UVI at the
 beginning of the lights-on or lights-off period. NeuN activity
 in Bexa-treated animals showed higher NeuN immunohisto-
 chemical expression whereas UVI exerted a decrease in the
 activity of this neuronal marker. These findings were observed
 when treatments were given at the beginning of the lights-on
 period. Conversely, when drugs were applied at the start of the
 dark period, we found that Bexa decreased the expression of
 NeuN while UVI increased the expression of NeuN if treat-
 ments were given at the start of the lights-on period. Taking
 together, our results demonstrated that RXR modulates the
 neuronal activity in hypothalamus as studied using NeuN im-
 munohistochemical procedures.

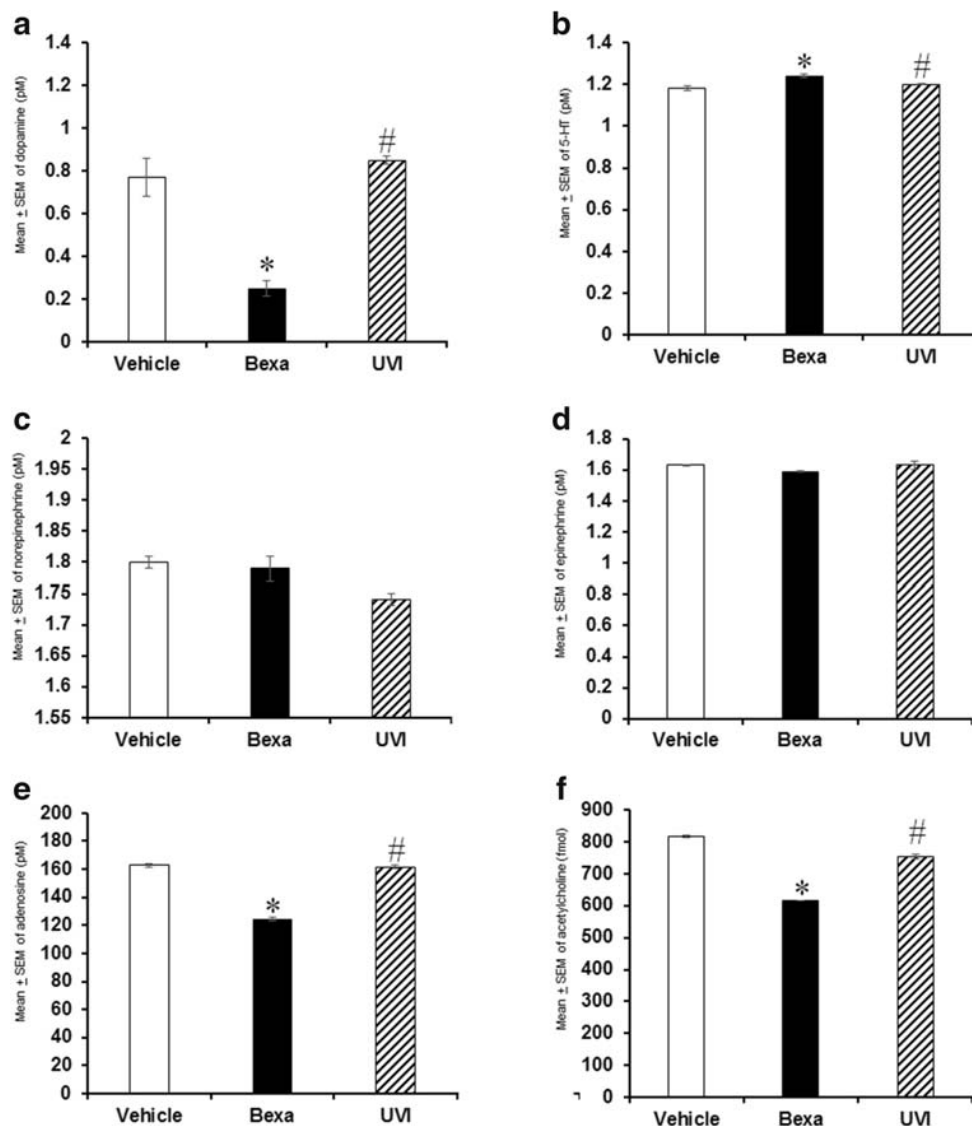


Fig. 6 The expression pattern of *c-Fos* in hypothalamus of rats that received bexarotene (Bexa) or UVI 3003 (UVI; 1 mM each compound) during either the lights-on or lights-off period. The dotted semicircle area in the schematic illustration from the rat brain atlas (Paxinos and Watson, 2005) shows the hypothalamus section taken for the immunohistochemical studies (coordinates -0.12 to -3.48 mm, from bregma according to the Rat Brain Atlas [Paxinos and Watson, 2005]; panel **a**). Compared with vehicle (panel **b**), Bexa (panel **c**) enhanced *c-Fos* expression in hypothalamus whereas UVI (panel **d**) caused opposite results when treatments were given at the beginning of the lights-on period. In comparison with vehicle (panel **e**), no differences were found in *c-Fos* expression in hypothalamus found in Bexa-treated rats (panel **f**)

or animals that received UVI (panel **g**) when given at the start of the lights-off period. The relative expression of *c-Fos* over the hypothalamus showed an enhancement in rats that received Bexa (panel **h**) whereas UVI caused an opposite effect (panel **h**) when compounds were given at the lights-on period ($P < 0.0007$; panel **h**). Bonferroni test showed differences among groups (VEH vs. Bexa, $P < 0.004$; VEH vs. UVI, $P < 0.05$; Bexa vs. UVI, $P < 0.0002$). Lastly, no statistical differences were found in *c-Fos* expression in hypothalamus after pharmacological treatments of either Bexa or UVI during the lights-off period ($P = 0.6$; panel **i**; *vs. control; #vs. Bexa). 3V, third lateral ventricle; CPu, caudate putamen (striatum); och, optic chiasm. Scale bar 100 μ m

Q2831 The RXR is a critical member of the superfamily of
 832 nuclear receptors that requires heterodimerization with
 833 peroxisome proliferator-activated receptors (PPAR) for
 834 binding to specific DNA sequences and activating genes
 835 to modulate multiple neurophysiological functions (Krężel
 836 et al., 2019; Kojetin et al., 2015; Lefebvre et al., 2010;;
 837 Schierle and Merk, 2019; Watanabe and Kakuta, 2018;
 838 Fig. 8). Thorough understanding of the functional role

of RXR in the control of a diversity neurobiological func-
 839 tions is crucial to determine the relevance of this nuclear
 840 receptor in controlling additional neurobiological vari-
 841 ables, including the sleep-wake cycle (Dheer et al.,
 842 2019; Guleria et al., 2013; Kojetin et al., 2015; Lefebvre
 843 et al., 2010; Loera-Valencia et al., 2019; Martin et al.,
 844 2019; Martínez et al., 2019; Mengeling et al., 2018;
 845 Simandi et al., 2018; Schierle and Merk, 2019). 846

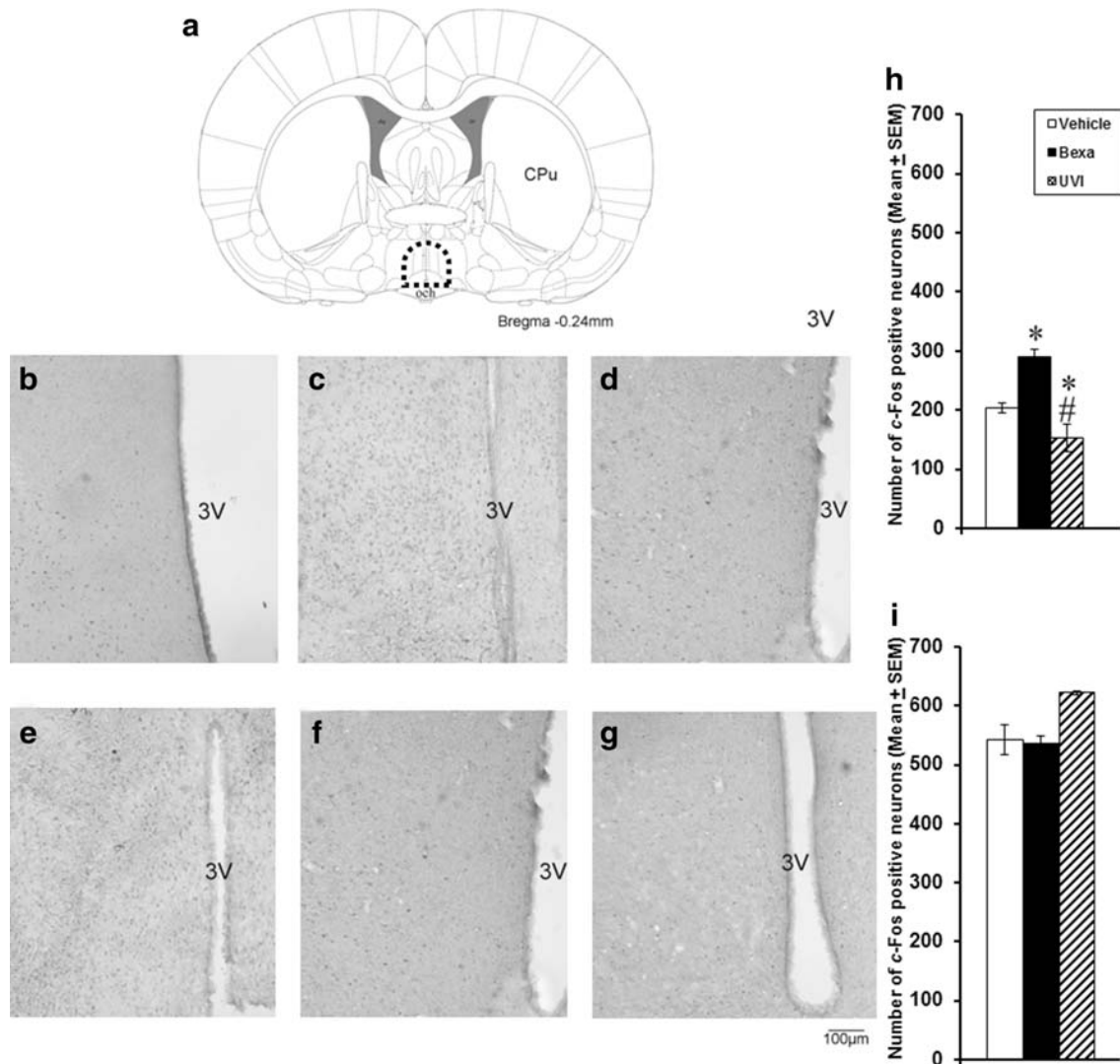


Fig. 7 The expression pattern of NeuN in hypothalamus of rats that received bexarotene (Bexa) or UVI 3003 (UVI; 1 mM each compound) during either the lights-on or lights-off period. Compared with vehicle (panel a), Bexa (panel b) enhanced *c-Fos* expression in hypothalamus whereas UVI (panel c) caused opposite results when experimental challenges were given at the start of the lights-on period. In contrast, in comparison with vehicle (panel d), NeuN expression in hypothalamus was decreased in Bexa-treated rats (panel e) while UVI enhanced NeuN activity (panel f) when treatments were given at the beginning of the dark phase. The relative expression of NeuN over the hypothalamus showed

an enhancement in rats that received Bexa (panel g) while UVI caused a contrary effect (panel g) when compounds were given at the lights-on period ($P < 0.0001$). Bonferroni test showed differences among groups (VEH vs. Bexa, $P < 0.0001$; VEH vs. UVI, $P < 0.0001$; Bexa vs. UVI, $P < 0.0001$). In addition, statistical differences were found in NeuN expression in hypothalamus after treatments given at the beginning of the lights-off period ($P < 0.0001$; panel h). Bonferroni test showed differences among groups (VEH vs. Bexa, $P < 0.0001$; VEH vs. UVI, $P < 0.0001$; Bexa vs. UVI, $P < 0.0001$; *vs. control; #vs. Bexa). 3V, third lateral ventricle. Scale bar 100 μ m

847 The role of PPAR in sleep modulation, as heterodimer partner of RXR, has been already studied. For example, previous pharmacological experiments have indicated that PPAR α participates in the control of the sleep-wake cycle since applications of synthetic agonist (Wy14643) of PPAR α in rats enhanced W and decreased SWS and REMS whereas the injection of the antagonist (MK-886) promoted opposite effects. Moreover, it has been demonstrated that injections of Wy14643 enhanced DA, NE, 5-HT, and AD levels collected from AcbC. In line with the idea that PPAR α participates in sleep control, the administration of natural

(oleoylethanolamide) or synthetic (Wy14643) ligand of PPAR α after 6 h of TSD showed a decrease in the sleep rebound, suggesting that PPAR α seems to modulate sleep homeostasis (Mijangos-Moreno et al., 2016; Murillo-Rodríguez et al., 2016; Murillo-Rodríguez, 2017). Since it was reasonable to argue that PPAR α might participate in the control of the sleep-wake cycle (Mijangos-Moreno et al., 2016; Murillo-Rodríguez et al., 2016; Murillo-Rodríguez, 2017), then RXR was, therefore, an ideal candidate to study its modulatory properties in sleep. Moreover, the role on sleep of RXR tested by the pharmacological administration of Bexa

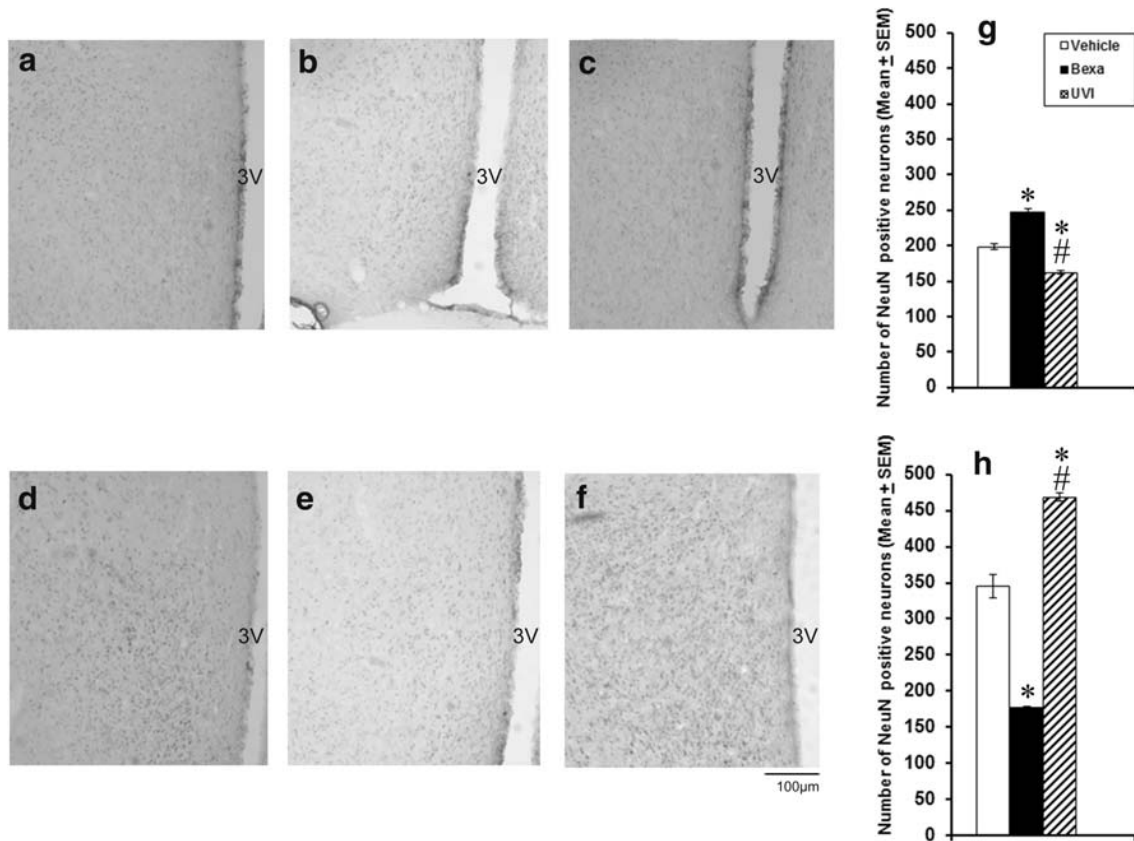


Fig. 8 Putative nuclear mechanism of action for RXR in sleep modulation. PPAR and RXR form a heterodimer, which is activated by their respective ligands for PPAR and RXR. Then, the activated

PPAR/RXR heterodimer is translocated into the nucleus for the regulation of downstream target genes related to sleep/neurochemical/*c-Fos*/NeuN control

869 or UVI was unknown. To overcome this limitation, in the
870 present study, we applied Bexa or UVI at either the start of
871 the lights-on or lights-off period, and sleep, sleep homeostasis,
872 neurochemicals linked to sleep control and the expression of
873 *c-Fos* and NeuN were analyzed.

874 Although it has been known that RXR modulates many
875 neurobiological processes (Bartzokis, 2014; Casali et al.,
876 2018; Clemens et al., 2018; Fanaee-Danesh et al., 2019;
877 Geller et al., 2019; Guleria et al., 2013; Hebert et al., 2017;
878 Loera-Valencia et al., 2019; Martin et al., 2019; McFarland
879 et al., 2013; Mengeling et al., 2018; Schierle and Merk, 2019;
880 Simandi et al., 2018; Tu et al., 2018; Watanabe and Kakuta,
881 2018), the mechanism of action is not fully understood. Thus,
882 our observations that Bexa or UVI modified the sleep archi-
883 tecture and sleep homeostasis might be linked with the chang-
884 es found in the neurochemical studies. However, there are
885 non-exclusive explanations for these findings. First, the mi-
886 crodialysis data suggest that RXR plays a crucial role for
887 modulating the extracellular levels of neurochemicals related
888 to the sleep-wake cycle. Although the results indicated that
889 Bexa and UVI controlled DA, 5-HT, NE, EP, AD, and ACh
890 contents during lights-on or lights-off period, it is likely that
891 Bexa or UVI could engage other neurobiological substrates
892 rather than the neurochemicals analyzed. In this regard,

893 Kitaoka et al. (2011) reported that chronic administration of
894 retinoic acid receptor antagonist, LE540 (30 mg/kg/day), dur-
895 ing 1 or 4 weeks decreased delta power during sleep as well as
896 attenuation of alertness. In addition, they found a significant
897 decrease in the expression of dopamine D1 receptor in the
898 striatum of treated animals as addressed by Western blot
899 means.

900 Second, the intense activation of neurons have been linked
901 to the activity of immediate expression genes, including *c-Fos*
902 since this gene is related to multiple signal cascades that are
903 involved in neurobiological processes and to mapping neuro-
904 nal activity (Farivar et al., 2004; Gallo et al., 2018; Huang
905 et al., 2019; Jaworski et al., 2018; Kovács, 2008; Yang et al.,
906 2019). In our study, we analyzed the *c-Fos* expression in a
907 brain area related to sleep modulation, the hypothalamus
908 (Arrigoni et al., 2019; Jones, 2019), and we found that Bexa
909 or UVI showed differential function activity. We surmise that
910 different brain areas could be under the influence of Bexa or
911 UVI as determined by changes in the levels of *c-Fos* marker.
912 Consistent with this view, ablation of RXR γ in mice leads to
913 *c-Fos* expression in dorsal caudate putamen (Krzyszosiak et al.,
914 2010). Due to the large number of brain nuclei related to sleep
915 control (Eban-Rothschild et al., 2018; Iovino et al., 2019),
916 identifying specific areas may reveal novel pathways for

917 understanding the relevant role of RXR in modulation of the
 918 states of vigilance. Importantly, we found that Bexa enhanced
 919 W during the lights-on period whereas UVI increased SWS
 920 during the lights-off period suggesting that the hypothalamus
 921 is reacting to compounds in a different pattern and depending
 922 on the time of the day as reported by others (Barros et al.,
 923 2015). We hypothesize that the expression of *c-Fos* in the
 924 hypothalamus after Bexa or UVI administrations might repre-
 925 sent a nuclear mechanism of action for sleep modulation and
 926 seems to be depending on the time of administration of
 927 compounds.

928 There is an assumption that NeuN is linked to neuronal
 929 functional state (Duan et al., 2016; Gusel'nikova and
 Q29 930 Korzhevskiy 2015). However, NeuN also may not be
 931 expressed at uniform levels within a specific brain region
 932 (Hight et al., 2010), meaning that a likely limitation of our
 933 study is that NeuN expression could be detected in a non-
 934 uniform fashion within the hypothalamus. In addition, it is
 935 worthy to highlight that our results showed a time-of-day ex-
 936 pression of NeuN after treatments. The activity dependency of
 937 NeuN in our experiments is consistent with the previous ob-
 938 servations (Geoghegan and Carter, 2008; Hight et al., 2010).
 939 Analyzing the role of NeuN in the activity of RXR could shed
 940 light on the neuromolecular basis of the sleep-wake cycle
 941 modulation by RXR. Indeed, further studies could provide a
 942 robust data linked to the mechanism of action of RXR and
 943 NeuN expression. We suspect that NeuN expression in ani-
 944 mals under treatment of Bexa or UVI is beyond than simple
 945 neuronal marker activity and it will require to be analyzed as a
 946 possible key participant in sleep modulation since this field
 947 has been completely unnoticed.

948 Finally, our understanding of the pharmacological effects
 949 of RXR isoforms is, in some cases, limited to in vitro assays.
 950 The elucidation of the neurobiological role of RXR isoforms
 951 has become an essential step in understanding how the RXR
 952 receptors modulate behaviors such as the sleep-wake cycle. In
 953 this regard, limited evidence is available about the role of
 954 RXR isoforms in the sleep control, sleep homeostasis regula-
 955 tion, as well as the modulation of neurochemicals and *c-Fos* or
 956 NeuN expression. The indirect evidence shows that the three
 957 PPAR isoforms display circadian rhythmicity in mouse tissues
 Q29 958 (Chen and Yang 2014), whereas PPAR α knockout mice dis-
 959 plays an increase in sleepiness (Kondo et al., 2020). Thus,
 960 further studies are required to fully elucidate the functions
 961 and potential mechanisms associated with RXR isoforms in
 962 sleep modulation.

963 In conclusion, by using Bexa or UVI, RXR activity mod-
 964 ified the sleep-wake cycle and sleep homeostasis dependent
 965 on the light/dark cycle. Our results also clearly showed that
 966 Bexa or UVI modulated the extracellular levels of neurochem-
 967 icals linked to sleep control whereas the expression of *c-Fos*
 968 and NeuN in hypothalamus showed different effects if treat-
 969 ments were given during either the lights-on or lights-off

period. Our data allow us to speculate that RXR might play 970
 a functional role in the modulation of the sleep-wake cycle. 971

Funding information This work was supported by the Escuela de 972
 Medicina, Universidad Anáhuac Mayab (PresInvEMR2018), given to 973
 E. MR. 974

Compliance with ethical standards 975

The experimental protocols were approved by the Research and Ethics 976
 Committee of Universidad Anáhuac Mayab (Mérida, Yucatán, México), 977
 and the protocols met the requirements of Animal Welfare including the 978
 Mexican Standards Related to Use and Management of Laboratory 979
 Animals (DOF. NOM-062-Z00-1999), the National Institutes of Health 980
 (NIH Publication No. 80-23, revised 1996), and the ARRIVE (Animal 981
 Research: Reporting of in vivo Experiments) guidelines, the commonly 982
 accepted “3Rs” Guidelines. 983
 984

Conflict of interest The authors declare that they have no conflict of 985
 interest. 986

References 987 Q24

AlSudais H, Aabed K, Nicola W, Dixon K, Chen J, Li Q (2018) Retinoid 988
 X receptor-selective signaling in the regulation of Akt/protein kinase 989
 B isoform-specific expression. *J Biol Chem* 293:9139. <https://doi.org/10.1074/jbc.AAC118.003993> 990
 991
 Anderzhanova E, Wotjak CT (2013) Brain microdialysis and its applica- 992
 tions in experimental neurochemistry. *Cell Tissue Res* 354:27–39 993
 Arrigoni E, Chee MJS, Fuller PM (2019) To eat or to sleep: that is a lateral 994
 hypothalamic question. *Neuropharmacol.* 154:34–49. <https://doi.org/10.1016/j.neuropharm.2018.11.017> 995
 996
 Barone R, Rizzo R, Tabbi G, Malaguamera M, Frye RE, Bastin J (2019) 997
 Nuclear peroxisome proliferator-activated receptors (PPARs) as 998
 therapeutic targets of resveratrol for autism spectrum disorder. *Int J* 999
Mol Sci 20:E1878. <https://doi.org/10.3390/ijms20081878> 1000
 Barros VN, Mundim M, Galindo LT, Bittencourt S, Porcionatto M, Mello 1001
 LE (2015) The pattern of *c-Fos* expression and its refractory period 1002
 in the brain of rats and monkeys. *Front Cell Neurosci* 9:72. <https://doi.org/10.3389/fncel.2015.00072> 1003
 1004
 Bartzokis G (2014) Inter-species glia differences: implications for suc- 1005
 cessful translation of transgenic rodent Alzheimer's disease model 1006
 treatment using bexarotene. *J Prev Alzheimers Dis* 1:46–50. <https://doi.org/10.14283/jpad.2014.20> 1007
 1008
 Blanco-Centurion C, Xu M, Murillo-Rodriguez E, Gerashchenko D, 1009
 Shiromani AM, Salin-Pascual RJ, Hof PR, Shiromani PJ (2006) 1010
 Adenosine and sleep homeostasis in the basal forebrain. *J* 1011
Neurosci 26:8092–8100 1012
 Casali BT, Reed-Geaghan EG, Landreth GE (2018) Nuclear receptor 1013
 agonist-driven modification of inflammation and amyloid pathology 1014
 enhances and sustains cognitive improvements in a mouse model of 1015
 Alzheimer's disease. *J Neuroinflammation* 15:43. <https://doi.org/10.1186/s12974-018-1091-y> 1016
 1017
 Chen L, Yang G (2014) PPARs integrate the mammalian clock and en- 1018
 ergy metabolism. *PPAR Res* 2014:653017. <https://doi.org/10.1155/2014/653017> 1019
 1020
 Chitranshi N, Dheer Y, Kumar S, Graham SL, Gupta V (2019) Molecular 1021
 docking, dynamics, and pharmacology studies on bexarotene as an 1022
 agonist of ligand-activated transcription factors, retinoid X recep- 1023
 tors. *J Cell Biochem In press.* <https://doi.org/10.1002/jcb.28455> 1024

- 1025 Choi CI (2019) Astaxanthin as a peroxisome proliferator-activated recep- 1091
 1026 tor (ppar) modulator: its therapeutic implications. *Mar Drugs* 17(4): 1092
 1027 E242. <https://doi.org/10.3390/md17040242> 1093
- 1028 Clemens V, Regen F, Le Bret N, Heuser I, Hellmann-Regen J (2018) 1094
 1029 Anti-inflammatory effects of minocycline are mediated by retinoid 1095
 1030 signaling. *BMC Neurosci* 19:58. <https://doi.org/10.1186/s12868-018-0460-x> 1096
 1031 1097
- 1032 de-la-Cruz M, Millán-Aldaco D, Soriano-Nava DM, Drucker-Colín R, 1098
 1033 Murillo-Rodríguez E (2018) The artificial sweetener Splenda intake 1099
 1034 promotes changes in expression of c-Fos and NeuN in hypothalamus 1100
 1035 and hippocampus of rats. *Brain Res* 1700:181–189. <https://doi.org/10.1016/j.brainres.2018.09.006> 1101
 1036 1102
- 1037 Dheer Y, Chitranshi N, Gupta V, Abbasi M, Mirzaei M, You Y, Chung R, 1103
 1038 Graham SL, Gupta V (2018) Bexarotene modulates retinoid-X- 1104
 1039 receptor expression and is protective against neurotoxic endoplasmic 1105
 1040 reticulum stress response and apoptotic pathway activation. *Mol Neurobiol* 55:9043–9056. <https://doi.org/10.1007/s12035-018-1041-9> 1106
 1041 1107
- 1042 Dheer Y, Chitranshi N, Gupta V, Sharma S, Pushpitha K, Abbasi M, 1108
 1043 Mirzaei M, You Y, Graham SL, Gupta V (2019) Retinoid x receptor 1109
 1044 modulation protects against ER stress response and rescues glaucoma 1110
 1045 phenotypes in adult mice. *Exp Neurol* 314:111–125. <https://doi.org/10.1016/j.expneurol.2019.01.015> 1111
 1046 1112
- 1047 Duan W, Zhang YP, Hou Z, Huang C, Zhu H, Zhang CQ, Yin Q (2016) 1113
 1048 Novel insights into NeuN: from neuronal marker to splicing regulator. 1114
 1049 *Mol Neurobiol* 53:1637–1647. <https://doi.org/10.1007/s12035-015-9122-5> 1115
 1050 1116
- 1051 Eban-Rothschild A, Appelbaum L, de Lecea L (2018) Neuronal mechanisms 1117
 1052 for sleep/wake regulation and modulatory drive. *Neuropsychopharmacol.* 43:937–952. <https://doi.org/10.1038/npp.2017.294> 1118
 1053 1119
- 1054 Fanaee-Danesh E, Gali CC, Tadic J, Zandl-Lang M, Carmen Kober A, 1120
 1055 Agujetas VR, de Dios C, Tam-Amersdorfer C, Stracke A, Albrecher 1121
 1056 NM, Manavalan APC, Reiter M, Sun Y, Colell A, Madeo F, Malle E, 1122
 1057 Panzenboeck U (2019) Astaxanthin exerts protective effects similar 1123
 1058 to bexarotene in Alzheimer's disease by modulating amyloid-beta 1124
 1059 and cholesterol homeostasis in blood-brain barrier endothelial cells. 1125
 1060 *Biochim Biophys Acta Mol basis Dis* 1865:2224–2245. <https://doi.org/10.1016/j.bbdis.2019.04.019> 1126
 1061 1127
- 1062 Farivar R, Zangenehpour S, Chaudhuri A (2004) Cellular-resolution 1128
 1063 activity mapping of the brain using immediate-early gene expression. 1129
 1064 *Front Biosci* 9:104–109 1130
 1065 1131
- 1066 Gallo FT, Katche C, Morici JF, Medina JH, Weisstaub NV (2018) 1132
 1067 Immediate early genes, memory and psychiatric disorders: focus 1133
 1068 on c-Fos, Egr1 and Arc. *Front Behav Neurosci* 12:79. <https://doi.org/10.3389/fnbeh.2018.00079> 1134
 1069 1135
- 1070 Geller S, Busam K, Hamlin PA, Moskowitz AJ, Horwitz SM, Myskowski 1136
 1071 PL (2019) Treatment of Rosai-Dorfman disease with oral 1137
 1072 bexarotene: a case series. *J Dermatol Treat* 30:503–505. <https://doi.org/10.1080/09546634.2018.1528001> 1138
 1073 1139
- 1074 Geoghegan D, Carter DA (2008) A novel site of adult doublecortin 1140
 1075 expression: neuropeptide neurons within the suprachiasmatic nucleus 1141
 1076 circadian clock. *BMC Neurosci* 9:2. <https://doi.org/10.1186/1471-2202-9-2> 1142
 1077 1143
- 1078 Guleria RS, Singh AB, Nizamutdinova IT, Souslova T, Mohammad AA, 1144
 1079 Kendall JA Jr, Baker KM, Pan J (2013) Activation of retinoid 1145
 1080 receptor-mediated signaling ameliorates diabetes-induced cardiac 1146
 1081 dysfunction in Zucker diabetic rats. *J Mol Cell Cardiol* 57:106– 1147
 1082 118. <https://doi.org/10.1016/j.yjmcc.2013.01.017> 1148
 1083 1149
- 1084 Gusel'nikova VV, Korzhhevskiy DE (2015) NeuN as a neuronal nuclear 1150
 1085 antigen and neuron differentiation marker. *Acta Nat* 7:42–47 1151
 1086 1152
- 1086 Hammarlund-Udenaes M (2017) Microdialysis as an important technique 1153
 1087 in systems pharmacology—a historical and methodological review. 1154
 1088 *AAPS J* 19:1294–1303. <https://doi.org/10.1208/s12248-017-0108-2> 1155
 1089 1156
- 1089 He J, Liu H, Zhong J, Guo Z, Wu J, Zhang H, Huang Z, Jiang L, Li H, 1157
 1090 Zhang Z, Liu L, Wu Y, Qi L, Sun X, Cheng C (2018) Bexarotene 1158
 1091 protects against neurotoxicity partially through a PPAR γ -dependent 1159
 1092 mechanism in mice following traumatic brain injury. *Neurobiol Dis* 117:114–124. <https://doi.org/10.1016/j.nbd.2018.06.003> 1160
 1093 1161
- 1094 Hebert SL, Fitzpatrick KR, McConnell SA, Cucak A, Yuan C, McLoon 1162
 1095 LK (2017) Effects of retinoic acid signaling on extraocular muscle 1163
 1096 myogenic precursor cells in vitro. *Exp Cell Res* 361:101–111. 1164
 1097 <https://doi.org/10.1016/j.yexcr.2017.10.007> 1165
 1098 1166
- 1098 Hight K, Hallett H, Churchill L, De A, Boucher A, Krueger JM (2010) 1167
 1099 Time of day differences in the number of cytokine-, neurotrophin- 1168
 1100 and NeuN-immunoreactive cells in the rat somatosensory or visual 1169
 1101 cortex. *Brain Res* 1337:32–40. <https://doi.org/10.1016/j.brainres.2010.04.012> 1170
 1102 1171
- 1102 Huang J, Liu F, Wang B, Tang H, Teng Z, Li L, Qiu Y, Wu H, Chen J 1172
 1103 (2019) Central and peripheral changes in FOS expression in schizo- 1173
 1104 phrenia based on genome-wide gene expression. *Front Genet* 10: 1174
 1105 232. <https://doi.org/10.3389/fgene.2019.00232> 1175
 1106 1176
- 1106 Huang SH, Zhang J, Li Y, Rong J, Wu ZK (2013) Time delay of micro- 1177
 1107 dialysis in vitro. *N Am J Med Sci* 5:149–152. <https://doi.org/10.4103/1947-2714.107540> 1178
 1108 1179
- 1108 Iovino M, Messana T, De Pergola G, Iovino E, Guastamacchia E, Giagulli 1180
 1109 VA, Triggiani V (2019) Vigilance states: central neural pathways, 1181
 1110 neurotransmitters and neurohormones. *Endocr Metab Immune Disord Drug Targets* 19:26–37. <https://doi.org/10.2174/1871530318666180816115720> 1182
 1111 1183
- 1111 Jaworski J, Kalita K, Knapska E (2018) c-Fos and neuronal plasticity: the 1184
 1112 aftermath of Kaczmarek's theory. *Acta Neurobiol Exp (Wars)* 78: 1185
 1113 287–296 1186
 1114 1187
- 1113 Jones BE (2019) Arousal and sleep circuits. *Neuropsychopharmacol.* 45: 1188
 1114 6–20. <https://doi.org/10.1038/s41386-019-0444-2> 1189
 1115 1190
- 1114 Kalinchuk AV, McCarley RW, Porkka-Heiskanen T, Basheer R (2011) 1191
 1115 The time course of adenosine, nitric oxide (NO) and inducible NO 1192
 1116 synthase changes in the brain with sleep loss and their role in the 1193
 1117 non-rapid eye movement sleep homeostatic cascade. *J Neurochem* 116:260–272. <https://doi.org/10.1111/j.1471-4159.2010.07100.x> 1194
 1118 1195
- 1115 Kho CM, Enche Ab Rahim SK, Ahmad ZA, Abdullah NS (2017) A 1196
 1116 review on microdialysis calibration methods: the theory and current 1197
 1117 related efforts. *Mol Neurobiol* 54:3506–3527. <https://doi.org/10.1007/s12035-016-9929-8> 1198
 1118 1199
- 1116 Kitaoka K, Shimizu M, Shimizu N, Chikahisa S, Nakagomi M, Shudo K, 1200
 1117 Yoshizaki K, Séi H (2011) Retinoic acid receptor antagonist LE540 1201
 1118 attenuates wakefulness via the dopamine D1 receptor in mice. *Brain Res* 1423:10–16. <https://doi.org/10.1016/j.brainres.2011.09.023> 1202
 1119 1203
- 1117 Kojetin DJ, Matta-Camacho E, Hughes TS, Srinivasan S, Nwachukwu 1204
 1118 JM, Cavett V, Nowak J, Chalmers MJ, Marciano DP, Kamenecka 1205
 1119 TM, Shulman AI, Rance M, Griffin PR, Bruning JB, Nettles KW 1206
 1120 (2015) Structural mechanism for signal transduction in RXR nuclear 1207
 1121 receptor heterodimers. *Nat Commun* 6:8013. <https://doi.org/10.1038/ncomms9013> 1208
 1122 1209
- 1118 Kondo Y, Chikahisa S, Shiuchi T, Shimizu N, Tanioka D, Uguisu H, Séi 1210
 1119 H (2020) Sleep profile during fasting in PPAR-alpha knockout mice. 1211
 1120 *Physiol Behav* 214:112760. <https://doi.org/10.1016/j.physbeh.2019.112760> 1212
 1121 1213
- 1119 Kou X, Chen G, Huang S, Ye Y, Ouyang G, Gan J, Zhu F (2019) In vivo 1214
 1120 sampling: a promising technique for detecting and profiling endog- 1215
 1121 enous substances in living systems. *J Agric Food Chem* 67:2120– 1216
 1122 2126. <https://doi.org/10.1021/acs.jafc.8b06981> 1217
 1123 1218
- 1120 Kovács KJ (2008) Measurement of immediate-early gene activation- c- 1219
 1121 fos and beyond. *J Neuroendocrinol* 20:665–672. <https://doi.org/10.1111/j.1365-2826.2008.01734.x> 1220
 1122 1221
- 1121 Krężel W, Rühl R, de Lera AR (2019) Alternative retinoid X receptor 1222
 1122 (RXR) ligands. *Mol Cell Endocrinol* 491:110436. <https://doi.org/10.1016/j.mce.2019.04.016> 1223
 1123 1224
- 1122 Krzyzosiak A, Szyszka-Niagolov M, Wietrzych M, Gobaille S, 1225
 1123 Muramatsu S, Krzel W (2010) Retinoid x receptor gamma control 1226
 1124 of affective behaviors involves dopaminergic signaling in mice. 1227
 1125 *Neuron*. 66:908–920. <https://doi.org/10.1016/j.neuron.2010.05.004> 1228
 1126 1229

1157 Laleh P, Yaser K, Alireza O (2019) Oleoylethanolamide: a novel pharmaceutical agent in the management of obesity-an updated review. *J Cell Physiol* 234:7893–7902. <https://doi.org/10.1002/jcp.27913>

1158

1159 Lefebvre P, Benomar Y, Staels B (2010) Retinoid X receptors: common heterodimerization partners with distinct functions. *Trends Endocrinol Metab* 21:676–683. <https://doi.org/10.1016/j.tem.2010.06.009>

1160

1161

1162

1163

1164 Loera-Valencia R, Goikolea J, Parrado-Fernandez C, Merino-Serrais P, Maioli S (2019) Alterations in cholesterol metabolism as a risk factor for developing Alzheimer's disease: potential novel targets for treatment. *J Steroid Biochem Mol Biol* 190:104–114. <https://doi.org/10.1016/j.jsmb.2019.03.003>

1165

1166

1167

1168

1169 Martin N, Ma X, Bernard D (2019) Regulation of cellular senescence by retinoid X receptors and their partners. *Mech Ageing Dev* 111131. <https://doi.org/10.1016/j.mad.2019.111131>

1170

1171

1172 Martínez C, Souto JA, de Lera AR (2019) Ligand Design for Modulation of RXR functions. *Methods Mol Biol* 2019:51–72. https://doi.org/10.1007/978-1-4939-9585-1_4

1173

1174

1175 McFarland K, Spalding TA, Hubbard D, Ma JN, Olsson R, Burstein ES (2013) Low dose bexarotene treatment rescues dopamine neurons and restores behavioral function in models of Parkinson's disease. *ACS Chem Neurosci* 4:1430–1438. <https://doi.org/10.1021/cn400100f>

1176

1177

1178

1179

1180 Mengeling BJ, Goodson ML, Furlow JD (2018) RXR ligands modulate thyroid hormone signaling competence in young *Xenopus laevis* tadpoles. *Endocrinol*. 159:2576–2595. <https://doi.org/10.1210/en.2018-00172>

1181

1182

1183

1184 Mijangos-Moreno S, Poot-Aké A, Guzmán K, Arankowsky-Sandoval G, Arias-Carrión O, Zaldívar-Rae J, Sarro-Ramírez A, Murillo-Rodríguez E (2016) Sleep and neurochemical modulation by the nuclear peroxisome proliferator-activated receptor α (PPAR- α) in rat. *Neurosci Res* 105:65–69. <https://doi.org/10.1016/j.neures.2015.09.005>

1185

1186

1187

1188

1189

1190 Mirza AZ, Althagafi II, Shamshad H (2019) Role of PPAR receptor in different diseases and their ligands: physiological importance and clinical implications. *Eur J Med Chem* 166:502–513. <https://doi.org/10.1016/j.ejmech.2019.01.067>

1191

1192

1193

1194 Murillo-Rodríguez E, Arankowsky-Sandoval G, Barros JA, Rocha NB, Yamamoto T, Machado S, Budde H, Telles-Correia D, Monteiro D, Cid L, Veras AB (2019) Sleep and neurochemical modulation by DZNep and GSK-J1: potential link with histone methylation status. *Front Neurosci* 13:237. <https://doi.org/10.3389/fnins.2019.00237>

1195

1196

1197

1198

1199

1200

1201

1202

1203

1204 Murillo-Rodríguez E, Di Marzo V, Machado S, Rocha NB, Veras AB, Neto GAM, Budde H, Arias-Carrión O, Arankowsky-Sandoval G (2017) Role of N-arachidonoyl-serotonin (AA-5-HT) in sleep-wake cycle architecture, sleep homeostasis, and neurotransmitters regulation. *Front Mol Neurosci* 10:152. <https://doi.org/10.3389/fnmol.2017.00152>

1205

1206

1207

1208

1209

1210 Murillo-Rodríguez E, Guzmán K, Arankowsky-Sandoval G, Salas-Crisóstomo M, Jiménez-Moreno R, Arias-Carrión O (2016) Evidence that activation of nuclear peroxisome proliferator-activated receptor alpha (PPAR α) modulates sleep homeostasis in rats. *Brain Res Bull* 127:156–163. <https://doi.org/10.1016/j.brainresbull.2016.09.007>

1211

1212

1213

1214

1215

1216 Murillo-Rodríguez E (2017) The role of nuclear receptor PPAR α in the sleep-wake cycle modulation. A tentative approach for treatment of sleep disorders. *Curr Drug Deliv* 14:473–482. <https://doi.org/10.2174/1567201814666161109123803>

1217

1218

1219

1220

1221

1222

1223

1224

1225

1226

1227

1228

1229

1230

1231

1232

1233

1234

1235

1236

1237

1238

1239

1240

1241

1242

1243

1244

1245

1246

1247

1248

1249

1250

1251

1252

1253

1254

1255

1256

1257

1258

1259

1260

1261

1262

1263

1264

1265

1266

1267

1268

1269

1270

1271

1272

1273

1274

1275

1276

1277

1278

1279

1280

1281

1282

1283

1284

1285

1286

levels in the basal forebrain of young and old rats. *Neurosci*. 123: 361–370

Nam KN, Mounier A, Fitz NF, Wolfe C, Schug J, Lefterov I, Koldamova R (2016) RXR controlled regulatory networks identified in mouse brain counteract deleterious effects of A β oligomers. *Sci Rep* 6: 24048. <https://doi.org/10.1038/srep24048>

Perrin-Terrin AS, Jeton F, Pichon A, Frugière A, Richalet JP, Bodineau L, Voituron N (2016) The c-FOS protein immunohistological detection: a useful tool as a marker of central pathways involved in specific physiological responses in vivo and ex vivo. *J Vis Exp*:110. <https://doi.org/10.3791/53613>

Porkka-Heiskanen T, Strecker RE, McCarley RW (2000) Brain site-specificity of extracellular adenosine concentration changes during sleep deprivation and spontaneous sleep: an in vivo microdialysis study. *Neurosci*. 99:507–517

Schierle S, Merk D (2019) Therapeutic modulation of retinoid X receptors - SAR and therapeutic potential of RXR ligands and recent patents. *Expert Opin Ther Pat* 29:605–621. <https://doi.org/10.1080/13543776.2019.1643322>

Sharma R, Sahota P, Thakkar MM (2017) Lesion of the basal forebrain cholinergic neurons attenuates sleepiness and adenosine after alcohol consumption. *J Neurochem* 142:710–720. <https://doi.org/10.1111/jnc.14054>

Simandi Z, Horvath A, Cuaranta-Monroy I, Sauer S, Deleuze JF, Nagy L (2018) RXR heterodimers orchestrate transcriptional control of neurogenesis and cell fate specification. *Mol Cell Endocrinol* 471: 51–62. <https://doi.org/10.1016/j.mce.2017.07.033>

Tu L, Yang XL, Zhang Q, Wang Q, Tian T, Liu D, Qu X, Tian JY (2018) Bexarotene attenuates early brain injury via inhibiting microglia activation through PPAR γ after experimental subarachnoid hemorrhage. *Neurol Res* 40:702–708. <https://doi.org/10.1080/01616412.2018.1463900>

Tunctan B, Kucukkavruk SP, Temiz-Resitoglu M, Guden DS, Sari AN, Sahan-Firat S (2018) Bexarotene, a selective RXR α agonist, reverses hypotension associated with inflammation and tissue injury in a rat model of septic shock. *Inflammation*. 41:337–355. <https://doi.org/10.1007/s10753-017-0691-5>

Vazquez-DeRose J, Schwartz MD, Nguyen AT, Warriar DR, Gulati S, Mathew TK, Neylan TC, Kilduff TS (2016) Hypocretin/orexin antagonism enhances sleep-related adenosine and GABA neurotransmission in rat basal forebrain. *Brain Struct Funct* 221:923–940. <https://doi.org/10.1007/s00429-014-0946-y>

Watanabe M, Kakuta H (2018) Retinoid X Receptor Antagonists. *Int J Mol Sci* 19:2354. <https://doi.org/10.3390/ijms19082354>

Wnuk A, Rzemieniec J, Lasoń W, Krzeptowski W, Kajta M (2018) Benzophenone-3 impairs autophagy, alters epigenetic status, and disrupts retinoid X receptor signaling in apoptotic neuronal cells. *Mol Neurobiol* 55:5059–5074. <https://doi.org/10.1007/s12035-017-0704-2>

Yamashita S, Masuda D, Matsuzawa Y (2019) Clinical applications of a novel selective PPAR α modulator, pemafibrate, in dyslipidemia and metabolic diseases. *J Atheroscler Thromb* 26:389–402. <https://doi.org/10.5551/jat.48918>

Yang H, Shan W, Zhu F, Yu T, Fan J, Guo A, Li F, Yang X, Wang Q (2019) C-Fos mapping and EEG characteristics of multiple mice brain regions in pentylentetrazol-induced seizure mice model. *Neurol Res* 41:749–761. <https://doi.org/10.1080/01616412.2019.1610839>

Yu XH, Zheng XL, Tang CK (2015) Peroxisome proliferator-activated receptor α in lipid metabolism and atherosclerosis. *Adv Clin Chem* 71:171–203. <https://doi.org/10.1016/bs.acc.2015.06.005>

Zhang Z, Zhao G, Liu L, He J, Darwazeh R, Liu H, Chen H, Zhou C, Guo Z, Sun X (2019) Bexarotene exerts protective effects through modulation of the cerebral vascular smooth muscle cell phenotypic transformation by regulating PPAR γ /FLAP/LTB $_4$ after subarachnoid

1287	hemorrhage in rats. Cell Transplant 963689719842161. https://doi.org/10.1177/0963689719842161	Neuroinflammation 16:47. https://doi.org/10.1186/s12974-019-1432-5	1293
1288			1294
1289	Zuo Y, Huang L, Enkhjargal B, Xu W, Umut O, Travis ZD, Zhang G, Tang J, Liu F, Zhang JH (2019) Activation of retinoid X receptor by bexarotene attenuates neuroinflammation via PPAR γ /SIRT6/FoxO3a pathway after subarachnoid hemorrhage in rats. J	Publisher's note Springer Nature remains neutral with regard to jurisdictional claims in published maps and institutional affiliations.	1295
1290			1296
1291			
1292			
1297			

UNCORRECTED PROOF

AUTHOR QUERIES

AUTHOR PLEASE ANSWER ALL QUERIES.

- Q1. Please check if all affiliations are presented correctly.
- Q2. Country name and city name have been provided for affiliation 2. Please check if correct.
- Q3. Several changes had been applied. Please check if the intended meaning was retained.
- Q4. Please check if the section headings are assigned to appropriate levels.
- Q5. Figure 1 was changed to Table 1. Please check.
- Q6. Please check if the modified sentence "The EEG/EMG data were characterized in wakefulness (W) when the presence of desynchronized EEG with high EMG activity was observed in sleep recordings..." retained the intended meaning.
- Q7. Ref. "Paxinos and Watson, 2005" is cited in the body but its bibliographic information is missing. Kindly provide its bibliographic information in the list.
- Q8. Please check if the modified sentence "The microdialysis sampling procedure was developed as previously reported" retained the intended meaning.
- Q9. Please check if the modified sentence "The HPLC procedure for detection of AD was developed as previously reported" retained the intended meaning.
- Q10. Please check if the modified sentence "As described in Experiment 4 with exception of aCSF which was composed by KCl..." retained the intended meaning and amend as deemed necessary.
- Q11. Please check if the modified sentence "The procedure to determine ACh was developed as previously reported..." retained the intended meaning and amend as deemed necessary.
- Q12. Ref. "Grupe et al., 2013" is cited in the body but its bibliographic information is missing. Kindly provide its bibliographic information in the list.
- Q13. Ref. "ZEN 2012" is cited in the body but its bibliographic information is missing. Kindly provide its bibliographic information in the list.
- Q14. Please check if the modified sentence "To determine the effect of RXR on sleep, Bexa or UVI was systemically..." retained the intended meaning and amend as deemed necessary.
- Q15. Figures were renumbered. Please check.
- Q16. Please check if all figure captions are presented correctly and amend as deemed necessary.
- Q17. The citation "Hammarlund-Udenaes, 2011" has been changed to "Hammarlund-Udenaes, 2017" to match the author name/date in the reference list. Please check if the change is fine in this occurrence and modify the subsequent occurrences, if necessary.
- Q18. Please check the sentence "On the other hand, when Bexa was injected at the start of the lights-off period, alertness was decreased and SWS was enhanced SWS..." for correctness.
- Q19. Please check if the modified sentence "Complementarily, UVI showed no significant..." retained the intended meaning.
- Q20. Please check if the modified sentence "The RXR is a critical member of the superfamily of nuclear receptors that requires heterodimerization with peroxisome proliferator-activated receptors (PPAR) for..." retained the intended meaning.
- Q21. Figures 5–9 contain poor-quality text inside the artwork. Please do not re-use the file that we have rejected or attempt to increase its resolution and re-save. It is originally poor; therefore, increasing the resolution will not solve the quality problem. We suggest that you provide us the original format. We prefer replacement figures containing vector/editable objects rather than embedded images. The preferred file formats are eps, ai, tiff, and pdf.
- Q22. The citation "Gusel'nikova et al., 2015" has been changed to "Gusel'nikova and Korzhevskiy, 2015" to match the author name/date in the reference list. Please check if the change is fine in this occurrence and modify the subsequent occurrences, if necessary.
- Q23.

AUTHOR'S PROOF!

The citation “Chen et al., 2014” has been changed to “Chen and Yang, 2014” to match the author name/date in the reference list. Please check if the change is fine in this occurrence and modify the subsequent occurrences, if necessary.

- Q24. Reference [Zuo et al, 2019] was provided in the reference list; however, this was not mentioned or cited in the manuscript. As a rule, all references given in the list of references should be cited in the main body. Please provide its citation in the body text.

UNCORRECTED PROOF